Elliptical polarization of Saturn Kilometric Radiation observed from high latitudes

Georg Fischer, Baptiste Cecconi, Laurent Lamy, Sheng-Yi Ye, Ulrich Taubenschuss, Wolfgang Macher, Philippe Zarka, William S. Kurth, Donald A. Gurnett

Elliptical polarization of Saturn Kilometric Radiation observed from high latitudes

G. Fischer,[1,2] B. Cecconi,[3] L. Lamy,[3] S.-Y. Ye,[2] U. Taubenschuss,[1] W. Macher,[1] P. Zarka,[3] W. S. Kurth,[2] and D. A. Gurnett[2]

Received 18 February 2009; revised 25 June 2009; accepted 25 June 2009; published 27 August 2009.

[1] The high-inclination orbits of the Cassini spacecraft from autumn 2006 until spring 2007 allowed the Cassini/RPWS (Radio and Plasma Wave Science) instrument to observe Saturn Kilometric Radiation (SKR) from latitudes up to 60° for the first time. This has revealed a surprising new property of SKR: above ~30° in observational latitude, a significant amount of SKR is strongly elliptically polarized, in marked contrast to previous observations from low latitudes, which showed only circular polarization. There are transitional latitudes where the elliptical polarization occurs in ''patches'' in the time-frequency spectrograms next to regions of still completely circularly polarized SKR. From ~45° to 60° in northern latitude, it is found that most of the SKR is elliptically polarized throughout its entire frequency range with an average degree of ~0.7 in linear polarization. We demonstrate the ellipticity of SKR by using the concept of ''apparent polarization'' in case of two-antenna measurements, but also show three-antenna measurements from which the polarization can be unambiguously determined. Possible reasons for the variation of SKR polarization with the observer's latitude will be discussed.

Citation: Fischer, G., B. Cecconi, L. Lamy, S.-Y. Ye, U. Taubenschuss, W. Macher, P. Zarka, W. S. Kurth, and D. A. Gurnett (2009), Elliptical polarization of Saturn Kilometric Radiation observed from high latitudes, *J. Geophys. Res.*, *114*, A08216, doi:10.1029/2009JA014176.

1. Introduction

[2] Saturn Kilometric Radiation (SKR) is known to be a strongly beamed nonthermal radio emission covering a frequency range from a few kHz up to 1.2 MHz and originating from auroral latitudes (see reviews by *Kaiser et al.* [1984] or *Zarka* [1998]). Since the detection of SKR by the PRA (Planetary Radio Astronomy) experiment onboard Voyager 1 [*Kaiser et al.*, 1980] it has been known that SKR is circularly polarized. The recorded SKR polarization during the two encounters with Saturn by both Voyagers suggested the existence of two distinct radio sources [*Warwick et al.*, 1981, 1982]. Right-handed (left-handed) polarized radiation is mainly observed by a spacecraft at northern (southern) latitudes. There are also regions at low latitudes (<10°) and beyond an equatorial shadow zone up to ~4 Saturn radii where both sources and hence both senses of polarization can be observed [*Lamy et al.*, 2008a]. It is widely accepted that SKR is generated by the cyclotron maser instability (CMI) process [*Wu and Lee*, 1979], where radio waves are generated close to the local gyrofrequency of precipitating electrons at Saturn's auroral magnetic field lines [*Galopeau et al.*, 1995]. The polarization characteristics suggest an emission in the right-hand extraordinary (R-X) mode with respect to the magnetic field, but marginal left-hand ordinary (L-O) mode SKR has also been detected recently [*Lamy et al.*, 2008b], albeit with an intensity 2–4 orders of magnitude below the R-X mode intensity [*Cecconi et al.*, 2009].

[3] The polarization measurements of SKR performed at low latitudes by Voyager/PRA [*Kaiser et al.*, 1984; *Ortega-Molina and Lecacheux*, 1990] as well as Cassini/RPWS [*Cecconi et al.*, 2006; *Lamy et al.*, 2008b] have shown that SKR is close to being a 100% circularly polarized radio emission with virtually no unpolarized or linearly polarized component. In this paper we show that this is not the case when SKR is observed from high spacecraft latitudes $|\lambda_{s/c}| > 30°$, and viewed from there SKR mostly exhibits a strong linear component, i.e., it is elliptically polarized. In section 2 we discuss how the Cassini/RPWS instrument can measure polarization using 2 or 3 antennas. We introduce the concept of apparent polarization, and in section 3 we further discuss this concept with regard to circularly and elliptically polarized radio waves. In section 4 we show spectra of apparent Stokes parameters from RPWS two-antenna measurements which reveal the elliptical polarization of SKR. This is confirmed in section 5 using three-antenna measurements, where we also show the error on source direction implied by the circular polarization hypothesis. In section 6 we analyze the occurrence of elliptically polarized SKR

[1]Space Research Institute, Austrian Academy of Sciences, Graz, Austria.
[2]Department of Physics and Astronomy, University of Iowa, Iowa City, Iowa, USA.
[3]LESIA, Observatoire de Paris, Meudon, France.

0148-0227/09/2009JA014176

with regard to spacecraft coordinates and evaluate how much of SKR is elliptical at higher latitudes. In the discussion (section 7) we shortly review the polarization characteristics of the nonthermal auroral radio emissions from other radio planets and discuss some possible reasons for the elliptical polarization of SKR. In Appendix A we derive the formulas for the apparent polarization for the RPWS instrument, and in Appendix B we discuss the influence of the background radiation on the measurement of circular polarization.

2. Measurement of Real and Apparent Polarization of Radio Waves With the Cassini/RPWS Instrument

[4] SKR intensities are measured by the High Frequency Receiver (HFR) of the RPWS instrument [*Gurnett et al.*, 2004]. SKR frequencies rarely go down to the frequency range of HFR band A (3.5–16 kHz), often SKR can be found in band B (16–71 kHz), and it is most intense in band C (71–319 kHz) and in the lower part of HF1 (typically 325 kHz–1.8 or 4.1 MHz). SKR is usually recorded in two different modes: RPWS either uses all of its 3 monopole antennas E_u, E_v, E_w to perform "direction-finding," or it uses only 2 antennas in a dipole-monopole mode (or polarimeter mode), where E_u and E_v form the dipole E_x, and E_w is the monopole. The three-antenna direction-finding (DF) mode has so-called goniopolarimetric capabilities (from *gonia*, Greek for angle), i.e., one can determine the direction of arrival of an incoming electromagnetic wave (given by the two angles θ and ϕ in a spacecraft fixed coordinate system), its flux S, as well as its polarization [*Cecconi and Zarka*, 2005]. The polarization is usually described by means of the Stokes parameters, with Q and U denoting the linear polarization and V the circular polarization [see, e.g., *Kraus*, 1986]. With the two-antenna dipole-monopole mode we obtain only 4 instantaneous measurements, which are the 2 autocorrelations (one for each antenna E_x and E_w), and the real and imaginary part of the cross correlation [*Vogl et al.*, 2004]. Equation (20) in the work of *Cecconi and Zarka* [2005] gives the system that has to be inverted to retrieve the wave parameters. Naturally, it is not possible to retrieve the 6 wave parameters (θ, ϕ, S, Q, U, V) from the 4 instantaneous measurement values of a two-antenna measurement, and we must make certain assumptions for at least two of these parameters.

[5] The first case is the so-called *polarimeter inversion*, where we make an assumption about the source direction (θ and ϕ), and the 4 other parameters (flux S and the 3 Stokes parameters Q, U, and V) can then be retrieved. This inversion was used by *Cecconi et al.* [2006] for SKR observed by RPWS from great distances during the Cassini inbound trajectory with the assumption that the source is Saturn. It was also used by *Fischer et al.* [2007] to determine the polarization of Saturn lightning radio emissions since a prominent cloud feature in Saturn's atmosphere could be identified as the source. The second case is the so-called *circular goniometer inversion* [*Cecconi and Zarka*, 2005], where it is assumed that the radio wave has no linear polarization, which means that $Q = U = 0$, and one can retrieve the incoming direction (θ, ϕ), the flux S, and the circular polarization V. This inversion has been used in the statistical study of SKR properties by *Lamy et al.* [2008b] as well as for the study of SKR source locations by *Cecconi et al.* [2009].

[6] From the polarimeter inversion one can retrieve the *real* polarization. It is given by the *Stokes parameters* which are defined via the wave electric field components in the *wave plane*, the plane perpendicular to the propagation vector. However, there is also another way to look at this problem with the concept of *apparent* polarization, which can be regarded as the polarization that is actually recorded by the 2 antennas. The *apparent* polarization is given by the *apparent Stokes parameters* q_{app}, u_{app}, v_{app}, which are defined by the wave electric field components measured by the 2 antennas in the *antenna plane*. The small letters and the index should indicate that we deal with normalized apparent Stokes parameters, which are divided by the apparent flux S_{app}, and therefore are scalars ranging from -1 to $+1$ with no physical units. The real polarization can be calculated from the apparent polarization by a linear transformation [see, e.g., *Hamaker et al.*, 1996; *Galopeau et al.*, 2007] in case the incoming wave direction is known. The formulas for the calculation of the apparent Stokes parameters are derived in Appendix A, and we note that the 2 antennas should be orthogonal (or close to it), which is actually the case for the RPWS antennas E_x and E_w. However, they need not have the same effective length. In sections 3 and 4 we plot SKR time-frequency spectra of the apparent flux S_{app}, the apparent circular polarization degree $d_{c,app} = v_{app}$, the apparent linear polarization degree $d_{l,app} = \sqrt{q_{app}^2 + u_{app}^2}$, as well as the apparent total polarization $d_{app} = \sqrt{q_{app}^2 + u_{app}^2 + v_{app}^2}$. The Voyager/PRA antenna system was actually measuring the apparent circular polarization v_{app} and not the real one. The concept of apparent polarization should become more clear in the next section, where we apply it to completely circularly and elliptically polarized waves.

[7] For more technical information about the RPWS antenna system and its HFR or the exact definition of the Cassini spacecraft frame we refer the reader to the instrument description by *Gurnett et al.* [2004]. For the HFR measurements and the effective length vectors of the RPWS antennas and their calibration see *Vogl et al.* [2004] or *Cecconi and Zarka* [2005]. We note that the antenna plane we mentioned previously is formed by the effective antenna axes and not by the physical antenna rods of the dipole E_x and the monopole E_w. A sketch of Cassini with this antenna plane was drawn in Figure 1 of *Fischer et al.* [2007], where also additional information on RPWS polarization measurements can be found.

3. Apparent Polarization of Circularly and Elliptically Polarized Radio Waves

[8] The apparent polarization of a completely circularly polarized wave can be understood most easily when one thinks about a circle projected onto a plane. The plane is the antenna plane, and the center of the circle is in this plane. The circle can be extended to a cylinder whose axis represents the wave propagation direction ($\vec{k}$-vector), and the tip of the wave electric field vector is rotating along the

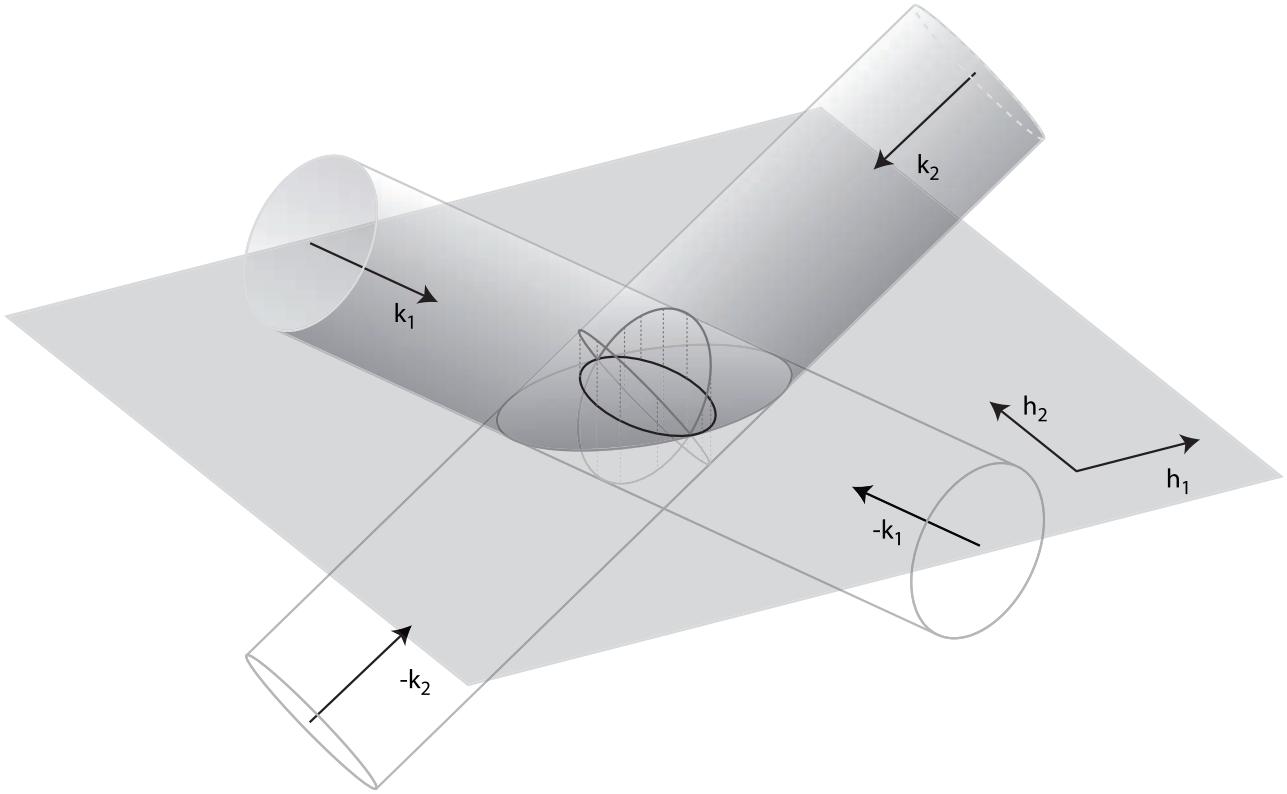

Figure 1. The apparent polarization is the polarization measured in the antenna plane, which is formed by the two effective length vectors $\vec{h}_1$ and $\vec{h}_2$. The vectors $\vec{k}_1$ and $\vec{k}_2$ are two independent wave vectors of circularly polarized waves giving the same observed apparent polarization ellipse. This ellipse is plotted in bold, and it is the result of a projection of the drawn circles onto the antenna plane. This also illustrates why the circular goniometer inversion has two solutions. (If the polarization sense is unknown, there are two more solutions, which are $-\vec{k}_1$ and $-\vec{k}_2$.)

circle. Figure 1 shows a sketch with such a situation, where two circularly polarized waves coming from two different directions intersect the antenna plane. In the general case the projection of the circles onto the plane forms an ellipse, whose major axis equals the diameter of the circle. There are two special cases: only if the $\vec{k}$-vector is perpendicular to the antenna plane, the circle will coincide with its own projection and the antenna system will measure a completely circularly polarized wave. If the radio source as well as the $\vec{k}$-vector are in the antenna plane, the circularly polarized wave will "appear" to the antenna system as a completely linearly polarized wave that is polarized perpendicular to the $\vec{k}$-vector in the antenna plane. In general, the degree of apparent linear polarization will decrease with increasing elevation of the radio source above the antenna plane. *Ortega-Molina and Daigne* [1984] have derived the following equation for the apparent circular polarization v_{app}:

$$v_{app} = \frac{2\cos(90^\circ - \beta)}{1 + \cos^2(90^\circ - \beta)} \frac{v}{1 - \frac{\sin^2(90^\circ - \beta)}{1 + \cos^2(90^\circ - \beta)} q} \qquad (1)$$

The angle β describes the elevation of the radio source with respect to the antenna plane, and v and q are the Stokes parameters of the *real* polarization of the incoming radio wave. (The wave frame can be rotated in such a way that $u = 0$ with all the linear polarization in the Stokes parameter q.) This equation can also be used if the wave is elliptically polarized, and for the case of a circularly polarized wave one simply sets $q = 0$.

[9] In Figure 2a (left) we have plotted v_{app} versus the angle β for 3 different cases: The first case with $v = 1$ and $q = 0$ represents a LH (left-handed) circularly polarized wave, the second case with $v = -1$ and $q = 0$ is a RH (right-handed) circularly polarized wave, and for the third case we have chosen arbitrarily $v = 0.53$ and $q = 0.85$ to plot an elliptically polarized wave. All 3 waves are completely polarized with no unpolarized part. It is clear from Figure 2 that the antenna plane bisects the space into 2 hemispheres, and one has to consider the 2 cases of positive and negative angle β. For $\beta > 0$ we have $sgn(v) = sgn(v_{app})$ (same sign of real and apparent circular polarization), whereas for $\beta < 0$, $sgn(v) = -sgn(v_{app})$. The latter means that a circularly polarized wave will appear to have the opposite polarization sense if the radio source lies in the hemisphere with $\beta < 0$. In case the radio source crosses the antenna plane due to a spacecraft rotation (or motion) there will be a sign flip in apparent circular polarization. For the E_x-E_w antenna plane of Cassini/RPWS the hemisphere with $\beta > 0$ is on the side on which the magnetometer boom is located ($+y$ hemisphere), whereas the cameras of the ISS (Imaging Science Subsystem) point toward the $-y$ hemisphere of

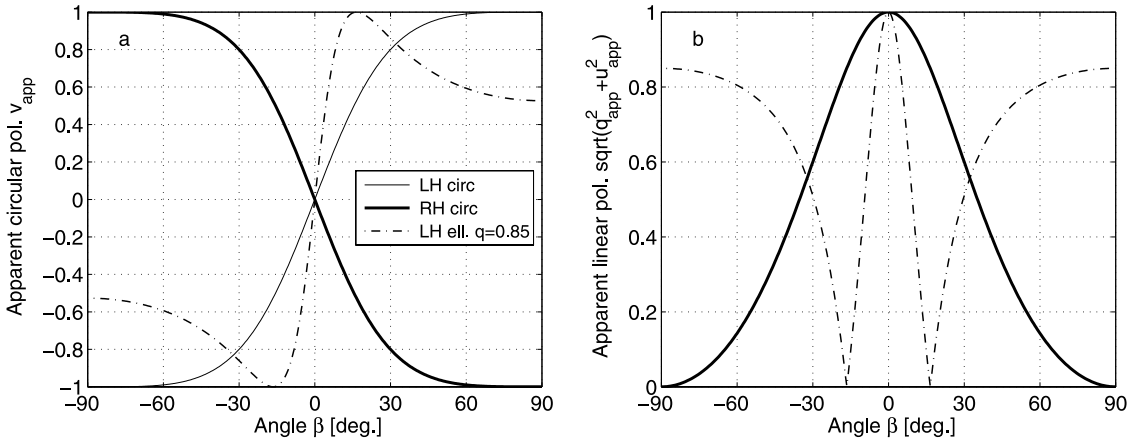

Figure 2. (a) Apparent circular polarization v_{app} and (b) apparent linear polarization $d_{l,app} = \sqrt{q_{app}^2 + u_{app}^2}$ as a function of the angle β (elevation of the radio source with respect to the antenna plane) for three different cases: a completely LH circularly polarized wave (solid line), a completely RH circularly polarized wave (thick solid line), and an elliptically polarized wave with real linear and circular polarizations given by the Stokes parameters $q = 0.85$ and $v = 0.53$, respectively (dash-dotted line). The completely LH and RH circularly polarized waves have the same apparent linear polarization (lines overlap).

$\beta < 0$ [see *Fischer et al.*, 2007, Figure 1]. Cassini frequently takes a position with ISS pointed toward Saturn and, assuming the center of Saturn is in the direction of the radio source, we have $\beta = -60.7°$. The E_x-E_w antenna plane can be described by its unit normal vector, which is given by $\vec{n}_{xw}$ = (−0.0079, 0.8720, −0.4894) in the Cassini spacecraft frame. This was calculated by using the calibrated effective length vectors of the RPWS antennas as given by *Vogl et al.* [2004, Table 5].

[10] In the case of a completely polarized wave like SKR [*Lamy et al.*, 2008b] the degree of apparent linear polarization $d_{l,app}$ can be calculated with the identity $d_{l,app} = \sqrt{1 - v_{app}^2}$, and we have plotted the theoretical function $d_{l,app} = d_{l,app}(\beta)$ in Figure 2b (right) for the same 3 cases as before. When the radio source passes through the antenna plane at $\beta = 0$ there is $v_{app} = 0$ and $d_{l,app} = 1$. We have observed this special behavior of SKR at numerous spacecraft rotations of Cassini, and one example is given in Figure 3. The antenna system cannot record any electrical component outside of the antenna plane, so a circularly polarized wave will be recorded as a linear polarized one at $\beta = 0$, since there is no phase shift between the two perpendicular components in the antenna plane. The dash-dotted lines in Figure 2 show the behavior in the case of an elliptically polarized wave. At an angle of $\beta \approx 16.5°$ there is the special case of $v_{app} = 1$ and $d_{l,app} = 0$. This can be easily understood as a polarization ellipse that is viewed from an angle at which it appears as a circle.

[11] Since Voyager's antenna system consists only of 2 antennas, it is only capable of measuring the apparent circular polarization and not the real one. For SKR the apparent circular polarization measured by Voyager/PRA did not reach ±1.0, because the direction to the radio source was generally not normal to the PRA antenna plane [*Kaiser et al.*, 1984]. Nevertheless, from the high degree of apparent circular polarization of SKR they concluded that SKR is 100% circularly polarized.

4. Apparent Polarization Spectra of SKR and Effects of Elliptical Polarization on Two-Antenna Goniopolarimetry

[12] With Cassini at a distance ∼18 R_S and at a latitude of ∼14° south we can see the apparent circular and linear polarization of SKR for 2 hours on DOY 034, 2007, as well as the angle β in the 3 left panels of Figure 3. We approximated the source elevation β by taking the angle β_S between the center of Saturn and the antenna plane, which should be a good approximation for a spacecraft that is relatively far from Saturn. Only from 9.33 to 9.97 SCET the angle β_S is positive, and the SKR appears LH polarized, which is also its real polarization sense since the spacecraft is located in the southern LH SKR domain of visibility [see *Lamy et al.*, 2008b, Figure 5]. In Figure 3 (right) we can see the apparent flux and total polarization, and the latter is very close to 1 indicating a completely polarized wave. (We note that for a completely polarized wave the real total polarization equals the apparent total polarization, and both are equal to 1.) In the SKR frequency range (20–1200 kHz) the background flux is only slightly varying with frequency and has a value of around −160 dB V^2/(Hz m^2). It will be shown in Appendix B that the signal has to be around 10 dB above the background, which is −150 dB V^2/(Hz m^2), to give reliable polarization measurements. In the case of Figure 3 the SKR behaves like a completely circularly polarized wave, and during the change in spacecraft attitude (and β) the apparent circular and linear polarization perfectly follow the theoretical behavior drawn in Figure 2. From Figure 2b we can see that for $|\beta| \approx 60°$ we should have $d_{l,app} \approx 0.15$, which is indicated by the blue color in the plot of apparent linear polarization of Figure 3.

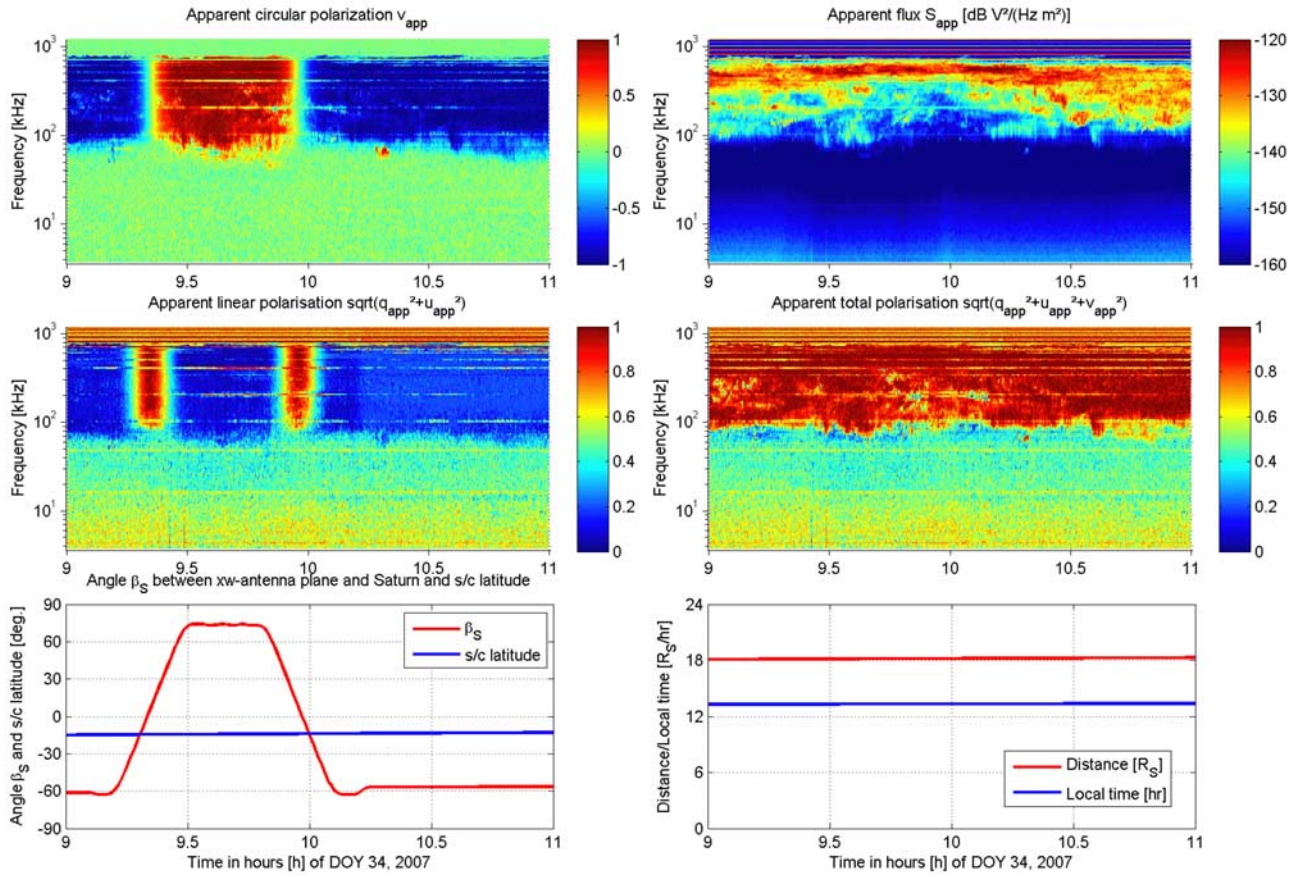

Figure 3. Apparent circular polarization, apparent flux, apparent linear, and total polarization (all color-coded) of SKR from 9 to 11 SCET (Spacecraft Event Time) on DOY 034, 2007, as a function of time and frequency. In the lower panels one can see the orbital parameters of Cassini, the latitude, the angle β_S between the center of Saturn and the E_x–E_w antenna plane, the distance, and the local time. All six panels have the SCET as x axis, but axes are only labeled in the two lower panels. In this example SKR behaves like a completely circularly polarized wave.

[13] In Figure 4 we have plotted the same apparent polarization spectra of SKR plus orbital parameters of Cassini for another time interval. Cassini is even further out at 26 R_S compared to Figure 3, and its local time is around midnight. The spacecraft latitude is ~38° north, and there is practically no change in spacecraft attitude, and β remains constant throughout the whole time interval of 3 hours. Its value is $\beta \approx \beta_S = -66°$ and from Figure 2b we infer that the apparent linear polarization for a circularly polarized wave should be quite low. It should be only $d_{l,app} \approx 0.09$, and thus there should be a similar blue tone in the plot of apparent linear polarization like in Figure 3. However, Figure 4 reveals a completely different picture. One can recognize a very patchy apparent linear polarization plot with regions of low and very high apparent linear polarization. The total polarization is still very high and close to 1, and in the regions of lower apparent linear polarization (~50–100 kHz in our example) the apparent circular polarization is higher. From Figure 2 it can be deduced that this unexpected behavior for SKR can be explained if one drops the hypothesis of complete circular polarization. The dash-dotted line in Figure 2b clearly indicates that an elliptically polarized wave can easily have a high degree of apparent linear polarization for high elevation angles, e.g., the drawn case has $d_{l,app} > 0.8$ for angles $|\beta| > 60°$. Note that for a fixed source elevation β above the antenna plane the apparent linear polarization (but not the real linear polarization!) does depend on the tilt angle of the polarization ellipse in the wave plane, hence a multitude of different values $d_{l,app}$ (as seen in Figure 4) is possible, in principle. This is not the case for a circularly polarized wave, which has a unique value of apparent linear polarization for a fixed source elevation. Hence any deviation from this unique value *must* be caused by an elliptically polarized wave.

[14] There is only one other possibility for explaining this high degree of apparent linear polarization, but we will argue below that this possibility is highly unlikely. A priori we do not know the exact position of the SKR source in our example, but we can make the following estimation. Many parts of the SKR from Figure 4 have $d_{l,app} \approx 0.8$, and assuming that SKR is completely circularly polarized we find from Figure 2b that in this hypothetical case the source elevation should be only around $|\beta| \approx 20°$. This deviates from the elevation of Saturn by ~46°, which corresponds to the minimum angle between the direction of Saturn and the supposed radio source. (The angle could be even larger since the 20° elevation is azimuthally symmetric around the antenna plane normal.) This means that the hypothetical

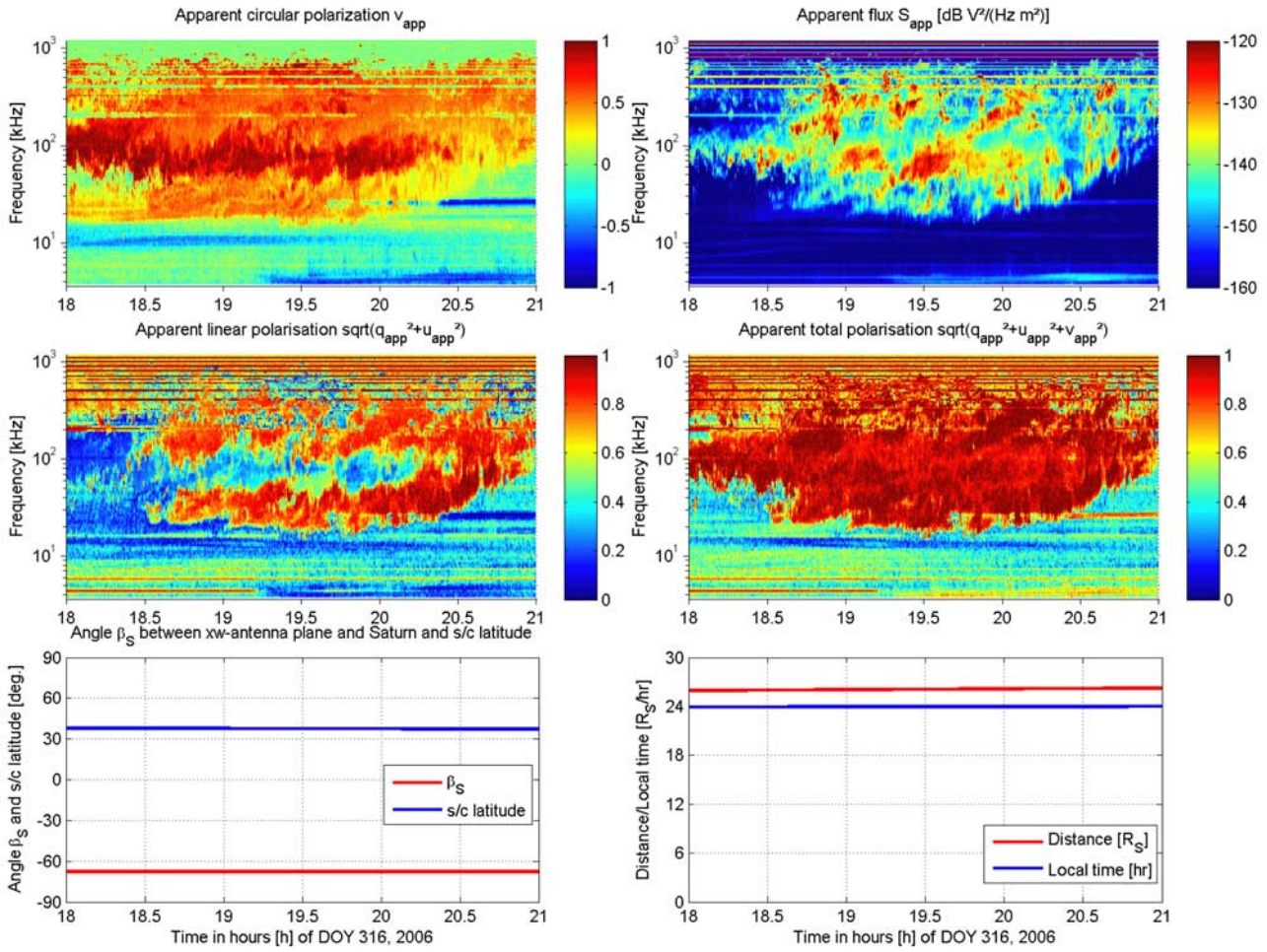

Figure 4. Apparent polarization spectra and orbital parameters of Cassini similar to Figure 3. The time goes from 18 to 21 SCET on DOY 316, 2006 and from the high apparent linear polarization at the constant angle of $\beta_S = -66°$ the real elliptical polarization of SKR is evident.

source direction is so far off from Saturn, that it can never intersect a surface of constant electron gyrofrequency (f_{ce}) corresponding to its frequency, which is easily shown by the following estimation: The maximum distance of the f_{ce} = 20 kHz isocontour from the center of Saturn is less than 4 R_S. Consequently, from the position of Cassini at 26 R_S, even the lowest SKR frequencies (see Figure 4) should only have a maximum angular distance from Saturn's center of $\arctan\left(\frac{4}{26}\right) \approx 9°$. Hence the solution with an angular offset $\geq 46°$ from Saturn is unphysical since it contradicts everything we know about SKR and its generation by the CMI mechanism in auroral regions. Furthermore, different degrees of apparent linear polarization like in Figure 4 would mean a multitude of different source directions both closer as well as further from Saturn. Since this makes no sense, we conclude that the SKR in Figure 4 does come from the auroral region of Saturn and is strongly elliptically polarized.

[15] The ellipticity of SKR has severe consequences on the applicability of the circular goniometer inversion. The prerequisite of no linear polarization is not fulfilled anymore. If it is nevertheless applied, it leads to a wrong Stokes parameter V and source directions far from Saturn, as described above. In Figure 5b it is illustrated that direction finding results for the two-antenna goniometer inversion (blue crosses) are far from Saturn in the case of elliptically polarized SKR. The only use for the circular goniometer inversion in this case is that it can serve as an indicator for the SKR ellipticity. The polarimeter inversion still can be used. Applying it with Saturn as preset source direction (especially from greater distances of Cassini) does, indeed, yield the ellipticity of SKR.

5. Three-Antenna Direction-Finding Measurements of Elliptically Polarized SKR

[16] Most of the time Cassini/RPWS records SKR using 2 antennas in its dipole-monopole mode. However, the three-antenna direction finding (DF) mode is also used on a regular basis. It allows the retrieval of the 6 wave parameters (θ, ϕ, S, Q, U, V) without any further assumption (there is only a 180° ambiguity in incoming wave direction). The RPWS three-antenna DF mode consists of two consecutive two-antenna measurements with different antenna pairs. Hence it is possible to apply a two-antenna direction finding inversion as well as a three-antenna inversion on

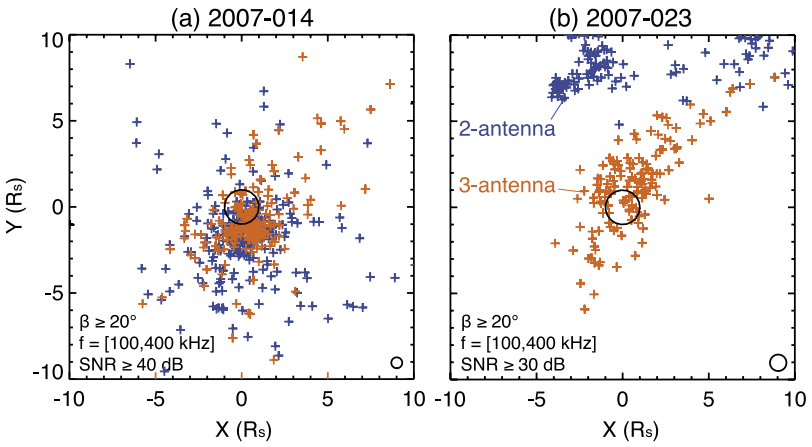

Figure 5. Direction-finding results of SKR projected onto a plane perpendicular to the line of sight toward Saturn (in the center). The two-antenna goniometer inversion (blue crosses) and the three-antenna direction finding inversion (orange crosses) are applied to three-antenna RPWS data of SKR. (a) Results from 04:35 to 13:33 SCET, DOY 014, 2007, with Cassini at a mean latitude of 20.2° south, a mean distance of 17.5 R_S, and a mean local time of 02:50. (b) Uses data from 03:38 to 12:30 SCET, DOY 023, 2007, with Cassini at a latitude of ~57° north, a distance of ~27.6 R_S, and a local time of ~21:30. Other data selection criteria regarding the angle β, the frequency, and the signal-to-noise ratio are indicated on the lower left side of each panel. Each cross corresponds to the auto and cross correlation measurements at one time at a certain SKR frequency. We selected only a few hundred measurements out of several hundred thousands. At the lower right side we indicate the theoretical error of direction finding of about 2°. However, the larger scattering of points could be due to extended or different sources, digitization errors, or refraction effects. We emphasize that similar direction finding results are gained with both inversions for circularly polarized SKR on the left side, whereas the two-antenna inversion results in incoming directions far off from Saturn for elliptically polarized SKR on the right side.

three-antenna data. Figure 5 shows two-dimensional maps of SKR direction-finding results projected on a plane perpendicular to the line of sight toward Saturn (in the center). The orange crosses were retrieved by a three-antenna inversion, whereas the blue crosses were retrieved by a two-antenna inversion applied on the same data. In Figure 5a Cassini is at an average latitude of 20.2° south, and both inversions show practically the same result. This indicates that this SKR must be completely circularly polarized since the two-antenna inversion makes the inherit assumption of no linear polarization. Conversely, in Figure 5b Cassini is at a latitude around 57° north, and the results of the two inversions strongly differ from each other. The three-antenna inversion still indicates a source close to Saturn as expected for SKR, whereas the two-antenna inversion shows non-realistic deviations from the direction of Saturn which were caused by the ellipticity of SKR that violates the no linear polarization assumption.

[17] Two examples showing the flux and the *real* linear polarization of SKR retrieved from three-antenna DF are displayed in Figure 6. The two spectra on the left side were recorded during a spacecraft roll-maneuver, which can be seen in the left bottom panel and by the vertical streaks of high linear polarization. When the source is close to the antenna plane of the used pair of antennas, the matrix equation for calculating the real polarization is very ill-conditioned resulting in a too high a degree of linear polarization. For a higher elevation of the source from the antenna plane ($|\beta| > 20°$ to 30°) this problem does not exist and the linear polarization should have the correct value. This is the case for limited time intervals during the roll-maneuver as well as throughout the time of the two spectra on the right side of Figure 6, where we have a constant attitude with $\beta_S \approx 61°$ (here the antenna plane is formed by the effective axes of the E_u and E_w antenna). In both examples there is a high degree of linear polarization, i.e., the SKR is again strongly elliptically polarized. However, at the same time there is also circularly polarized SKR in the second example around 09:30 SCET and 40 kHz.

[18] In Figure 7 we present a more comprehensive investigation of SKR polarization of three-antenna DF data recorded by RPWS between DOY 013 and 026, 2007. This period of time corresponds to a high inclination orbit covering latitudes of nearly up to 60° north and south. Figure 7 consists of three rows showing the results for three different observational latitude intervals of Cassini, which are 0°–20°, 20°–40°, and 40°–60° (both north and south). In the first column we plotted the degree of real circular polarization versus the signal-to-noise ratio (SNR) when we apply the two-antenna circular goniometer inversion on one antenna pair when the HFR is in three-antenna DF mode. As already mentioned, this inversion principally fails for elliptically polarized radio waves, and one can see that the real circular polarization is close to ±1.0 for all three observational latitude ranges of Cassini. Only the full three-antenna inversion reveals the correct polarization properties, and we plot the real circular and linear polarization of SKR in the second and third column, respectively. In the 20°–40°

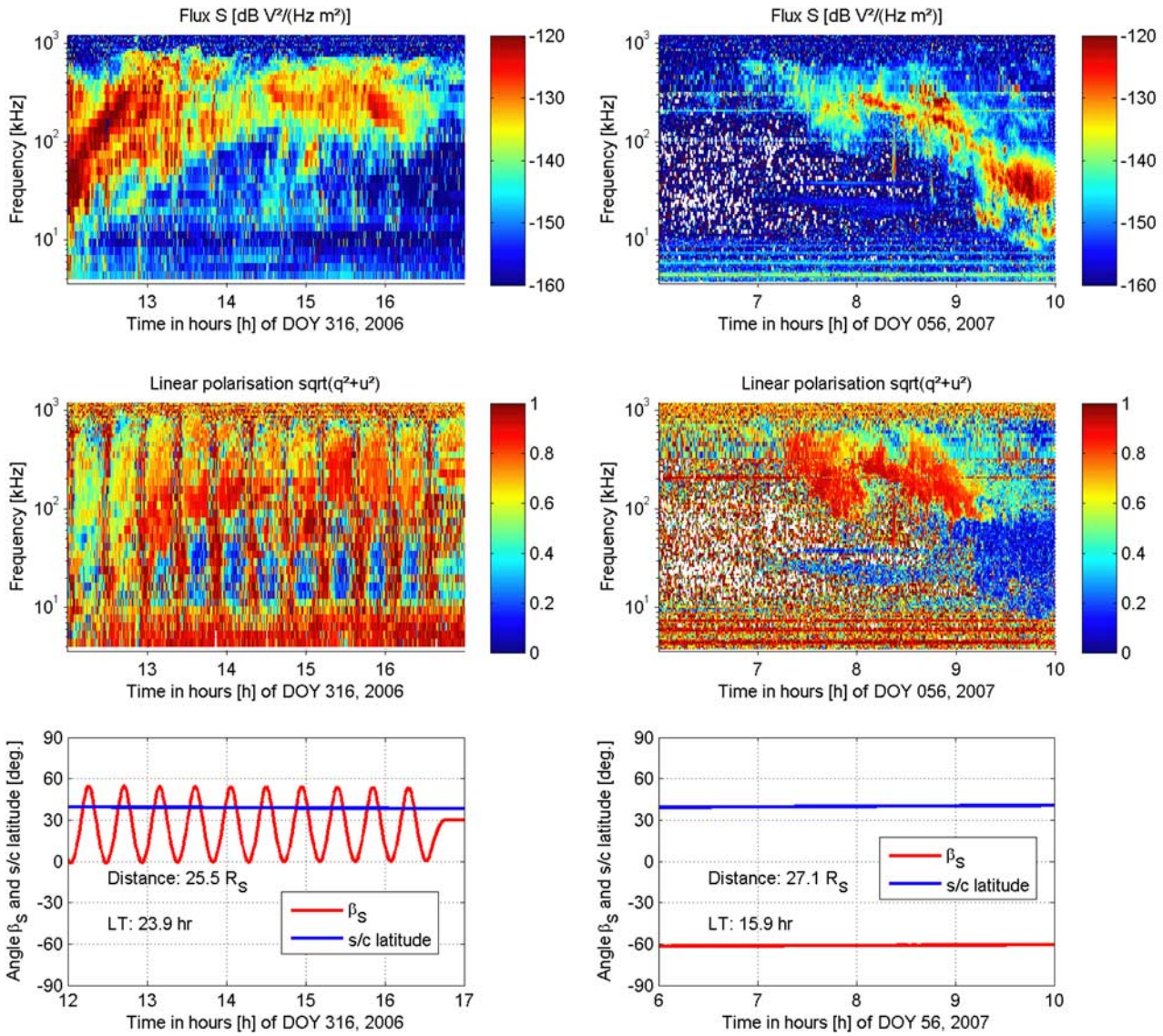

Figure 6. Two examples of flux and linear polarization spectra retrieved from RPWS three-antenna direction finding showing elliptically polarized SKR. At the bottom the spacecraft latitude as well as the angle β_S between the center of Saturn and in this case the E_u–E_w antenna plane are given. Additionally the mean spacecraft distance and local time are noted, which both do not change significantly within the respective time interval.

latitude interval (second row) one can see that practically all values of linear polarization from 0 to 1 are present indicating that elliptically polarized SKR as well as completely circularly polarized SKR are both present (like in Figure 4). This is different for the high latitude interval of 40°–60° (third row), where very few completely circularly polarized SKR can be found. Here the magnitude of the circular polarization $|v|$ covers a range from ~0.3 to ~0.8 and the linear polarization d_l from ~0.6 to ~1. Typical values are indicated by the arrows, e.g., $v \approx -0.5$ (RH SKR from northern hemisphere) and $d_l \approx 0.87$. The spreading in v and d_l below 10–13 dB SNR is due to the fact that this is the background intensity region, where the applied background subtraction causes an arbitrary polarization (see also Appendix B).

6. Occurrence of Elliptical Polarization of SKR

[19] The Cassini spacecraft started to go on higher latitude orbits on July 22 (DOY 203), 2006, and it returned to Saturn's equatorial plane on June 13 (DOY 164), 2007. On 25 September (DOY 268) 2006, the inclination exceeded 30° for the first time, and it returned to orbits below a maximum latitude of 30° in magnitude on 11 May (DOY 131) 2007. In the following we investigate the occurrence of elliptically polarized SKR from 1 September 2006 (DOY 244) until 31 May 2007 (DOY 151), which are

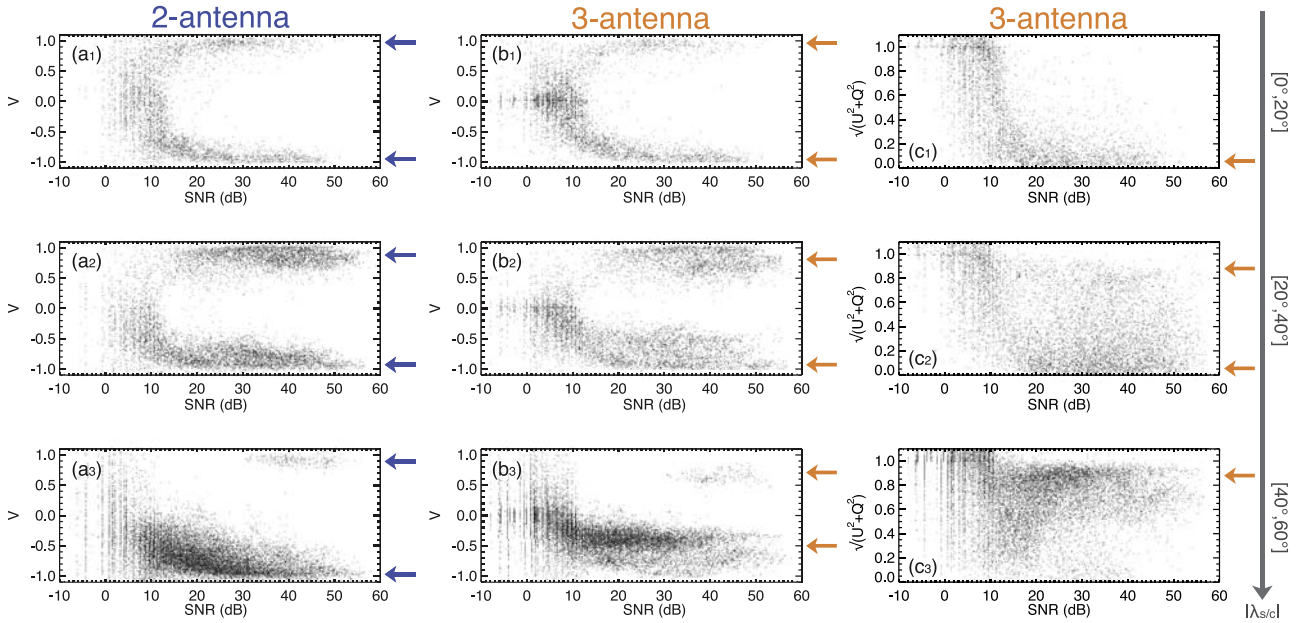

Figure 7. SKR polarization computed between 13 and 26 January 2007. Two-antenna and three-antenna inversions were used when the HFR was in three-antenna mode. The selected frequency range is 100–200 kHz. Columns (a), (b), and (c) show v (2 ant.), v (3 ant.) and $\sqrt{u^2+q^2}$ versus SNR on the E_w antenna, respectively. Using the SNR on the E_u or E_v antenna would give similar results. Rows (1), (2), and (3) show the results for the following spacecraft absolute latitude intervals: $|\lambda_{s/c}|$ in [0°, 20°], [20°, 40°], [40°, 60°]. The arrows indicate typical values for high SNR values, and one data point corresponds to one time-frequency measurement like in Figure 5.

273 days. Typically, RPWS was in three-antenna DF mode for 8–9 hours per day, and the rest was two-antenna mode. Only for about 40 days of this time interval RPWS used no or very few DF mode resulting in a coverage of about 30% with DF mode. Data coverage was nearly continuous, there were only a few longer data gaps (half-day gaps on DOY 287, 2006; DOY 052, 053, 2007; and nearly no measurements on DOY 093, 094, 2007). From 1 September 2006 until 31 May 2007 Cassini was on the orbits 28–45. It made 18 periapsis passes, 36 ring plane crossings, and 18 excursions to higher northern and southern latitudes, respectively. The Cassini trajectory went through the so-called 180° transfer, during which the local time of apoapses and periapses changed significantly. The apoapses took place with Cassini at high northern latitudes, and their local time changed from around midnight in autumn 2006 to afternoon in spring 2007. The periapsis passes took place in high southern latitudes around noon local times in 2006 and changed to early morning in 2007. In Figures 8 and 9 we plot the position of Cassini when it measured elliptically polarized SKR in equatorial and meridional views, respectively. In the meridional view of Figure 9 one can clearly see that elliptically polarized SKR is restricted to high observational latitudes, and we also indicate the latitude of 30°, which represents a reasonable boundary latitude above which elliptically polarized SKR is observed. There are only a few cases at greater distances of Cassini where elliptically polarized SKR can be found at slightly lower latitudes down to about 25°. In the equatorial view of Figure 8 one can note the absence of elliptically polarized SKR in the local time (LT) intervals of ~01–03 LT and ~13–15 LT. However, this is only a sampling effect of the spacecraft trajectory since Cassini was never located at latitudes exceeding 30° in magnitude in these two local time intervals. (From September 2006 until May 2007 all descending ring plane crossings took place between 2.4 and 1.6 LT, and all ascending ring plane crossings were from 14.3 to 13.6 LT.) Hence there is most likely no local time

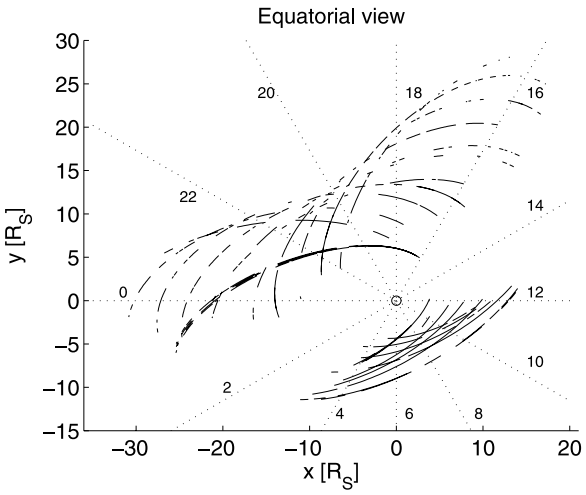

Figure 8. Position of Cassini during occurrence of elliptically polarized SKR from September 2006 until May 2007 in equatorial view. The Sun is toward positive x in the plane formed by Saturn's rotation axis and the x axis. The dotted lines with the numbers are drawn to indicate the local time for every 2 h.

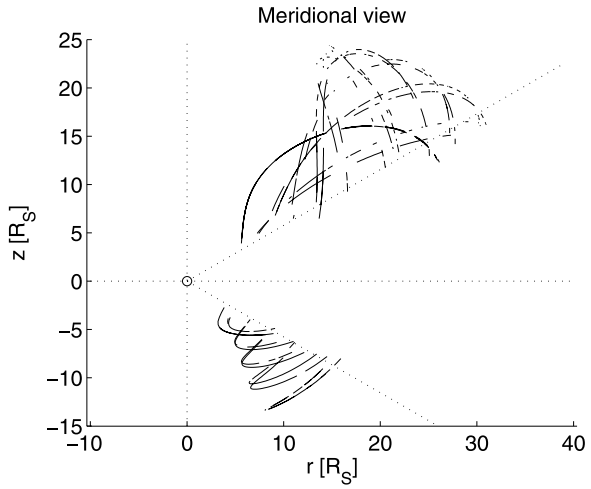

Figure 9. Position of Cassini during occurrence of elliptically polarized SKR from September 2006 until May 2007 in meridional view. Saturn's rotation axis (z axis), its equatorial plane ($z = 0$), and the latitudes of ±30° are indicated by dotted lines.

preference for the occurrence of elliptically polarized SKR. Besides those two big gaps in local time, there are also many smaller gaps in occurrence of elliptical SKR at higher latitudes. These gaps are either due to no or only weak SKR emissions or due to spacecraft attitudes where Saturn is in or close to the antenna plane. In both cases it is not possible to decide whether elliptically polarized SKR is present or not.

[20] We used three-antenna as well as two-antenna RPWS data to search for elliptically polarized SKR as plotted in the previous two figures. For each hour from 1 September 2006 until 31 May 2007 we determined the number of data points that were considered as due to elliptically polarized SKR by the following criteria: They were in the frequency range from 50 to 1200 kHz, their signal-to-noise ratio (SNR) was greater than 23 dB, and their apparent linear polarization deviated by more than 0.2 from the expected value. The latter was determined by calculating the angle β and using the equations from section 3. The choice of the low limit of 50 kHz for the frequency range excludes possible Saturn narrowband radio emissions from the analysis. The SNR threshold of 23 dB was set because the apparent polarization was calculated without background subtraction, and it is shown in Appendix B that in this case the polarization is correctly measured only for strong signals. In the spectra of Figures 3, 4, and 6 one can see some horizontal lines which are instrumental inferences. They typically show a higher linear polarization, and such frequency channels were simply excluded from the analysis. The deviation of 0.2 from the expected value of apparent linear polarization can be justified in the following way. The standard deviation $\sigma_{l,app}$ of the apparent linear polarization $d_{l,app}$ for many data points of circularly polarized SKR is typically $\sigma_{l,app} \approx 0.05$. Hence with a deviation greater than 0.2 (corresponding to $4\sigma_{l,app}$ from the expected value) one can be relatively sure that such data points are due to elliptically polarized SKR. When Cassini was in the northern (southern) hemisphere exceeding a spacecraft latitude of 15°, an average northern (southern) SKR source located 1 R_S above the north (south) pole (2 R_S from Saturn's center) was taken for the calculation of the angle β (otherwise the center of Saturn was taken). Each hour of Cassini's trajectory was now considered as an hour containing elliptically polarized SKR only in case if more than 1000 data points and more than 20% of all SKR data points within that hour had a higher apparent linear polarization (by 0.2) than expected. In this way Figures 8 and 9 were created.

[21] In Figure 10 we plot the (real) linear polarization of SKR and the spacecraft latitude as a function of time from DOY 013 to DOY 042, 2007. In this time interval Cassini makes nearly 2 orbits (orbit 37 and 38) around Saturn with 2 relatively distant periapsis passes around 12 and 15 R_S, respectively. The mean linear polarization d_l in Figure 10 denotes the mean linear polarization of all SKR data points (from 50 to 1200 kHz in frequency and with SNR > 23 dB)

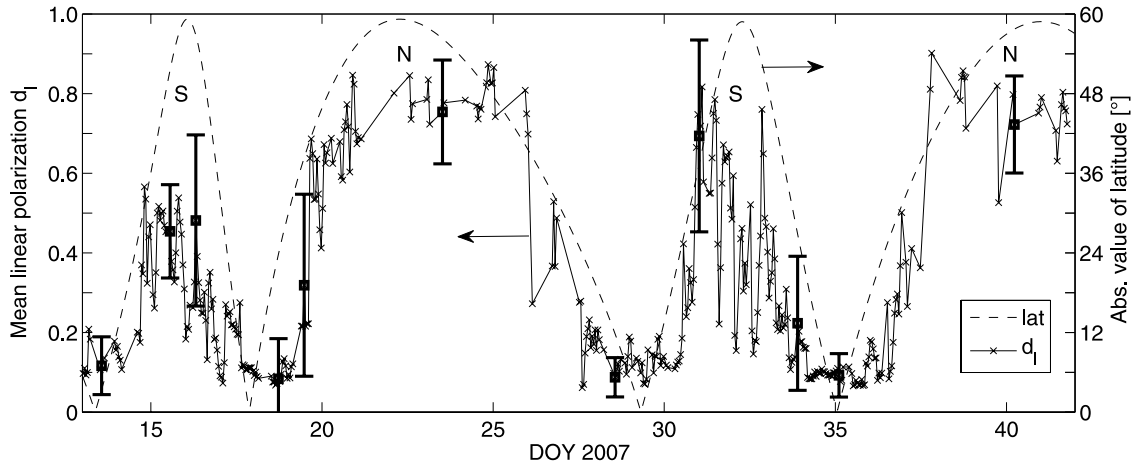

Figure 10. Mean linear polarization d_l of SKR (left y axis) and Cassini spacecraft latitude (absolute value $|\lambda_{s/c}|$, right y axis) as a function of day of year 2007. The SKR data points with SNR > 23 dB and from 50 to 1200 kHz were taken to calculate a mean value for d_l for each hour. "N" and "S" indicate when Cassini was located in the northern and southern hemisphere, respectively. For illustration the standard deviations (error bars) are drawn with bold lines and square markers for a few points only.

of each hour. Since the calculation of the linear polarization by the polarimeter inversion has high errors when the incoming wave direction is close to the antenna plane, we excluded all SKR data points with an incoming wave direction within 30° of the antenna plane. We also plot the absolute value of the latitude of Cassini (right *y* axis) as a function of time, where the two narrow humps are southern latitudes and the two broader humps are northern latitudes since Cassini spent more time in the northern hemisphere. It is also obvious from this plot that the linear polarization is higher at higher observational latitudes and reaches values around $d_l \approx 0.8$ for the northern hemisphere. The passage of Cassini through high southern latitudes is shorter in time and usually takes place at closer distances to Saturn. For the two southern passes of Cassini in Figure 10 the linear polarization of all SKR data points is somewhat smaller and more varying. At low latitudes the linear polarization is typically around 0.1, which should be close to the error for linear polarization determination.

[22] The typical standard deviation for the apparent linear polarization measurements is $\sigma_{l,app} \approx 0.05$. This error comes mainly from the digitization error and the calibration error for the ratio of the effective lengths (see the equations in Appendix A). However, for the calculation of real linear polarization one has to take the relative geometry of the antenna system with respect to the source into account. This transformation will somewhat increase the error, due to the error in incoming wave direction and antenna calibration. Under the prerequisites of high SNR and $|\beta| > 20°$ *Cecconi and Zarka* [2005] found an error of $\sigma_{l,real} \approx \pm 0.1$ for linear polarization measurements. There is also a bias toward linear polarization simply due to the formula $d_l = \sqrt{q^2 + u^2}$ with which it is calculated. We measure the Stokes parameters q and u that can be positive or negative, and which are clustered around zero for a circularly polarized wave. Small deviations (measurement errors) of Δq and Δu translate to small positive values of linear polarization even when the mean values $\overline{q}$ and $\overline{u}$ are practically zero indicating no linear polarization. Hence on the contrary to *Galopeau et al.* [2007] we do not interpret such low values of linear polarization as being due to elliptically polarized SKR. In Figure 10 we have drawn a few points with error bars, calculated as the standard deviations of the linear polarization measurements of SKR data points within one hour. At low latitudes and high northern latitudes the error is typically ±0.1 as outlined above. For some data points the error is higher around ±0.2. We will show in the following that this is not due to a higher measurement error, but due to the simultaneous existence of circularly and elliptically polarized SKR regions (see Figure 4) at so-called "transitional" latitudes.

[23] Other criteria can also be used as indicators of elliptically polarized SKR. One can use the circular goniometer inversion and elliptically polarized SKR is present if the source direction is more than 20° off from Saturn. Furthermore, the polarimeter inversion with a preset source direction in the direction of the center of Saturn and a threshold for the linear polarization of 0.2 can be applied as an indicator for elliptically polarized SKR. In Figure 11 these two methods (black line and gray line, respectively) were used to estimate the percentage of data points of circularly polarized SKR as a function of latitude, local time, and distance. The data from 1 September 2006 until 31 May 2007 was investigated with the selection criteria of a frequency interval from 100 to 1200 kHz, a SNR > 30 dB, an elevation above the antenna plane of $|\beta| > 30°$, and a circular polarization $|v| < 1.1$. For latitudes below 25°–30° in magnitude almost all SKR is completely circularly polarized and the dip (in the southern hemisphere) can probably be explained by the imperfection of the two criteria at close distances to Saturn. From ~30° to 45° northern latitude there is a transitional region, in which circularly polarized SKR coexists with elliptically polarized SKR similar to the spectra shown in Figures 4 and 6. For southern latitudes this transitional region goes up to ~60°, so there is a certain hemispherical asymmetry. At higher northern latitudes from ~45° to 60° there are only a few circularly polarized SKR events and most of the SKR is elliptically polarized throughout its entire frequency range. In the apparent polarization spectra we found elliptically polarized SKR at very low frequencies of a few kHz as well as up to its upper frequency limit around 1 MHz. This means that SKR sources far away from Saturn as well as those close to Saturn can be elliptically polarized. Sometimes, SKR exhibits an arc-like structure in the dynamic spectrum [*Boischot et al.*, 1981; *Lamy et al.*, 2008a], and such arcs can be also identified in the spectra of apparent linear polarization, i.e., certain arcs show a similar elliptical polarization. This can be partly seen in Figure 4, e.g., the region around 200 kHz and 20 SCET (lower left and upper right from this point) shows a high apparent linear polarization. The second and third panel of Figure 11 show the circularly polarized data samples fraction (in short CPF) as a function of local time and distance, respectively. The middle panel of Figure 11 shows dips in the percentage of circularly polarized SKR data points when Cassini is on the morning side around 07 LT and on the early night side around 21 LT. Again, this is a trajectory effect because the excursion to higher latitudes are also around such local times. Cassini was below 30° south only at local times from 3.2 to 12.5 LT and above 30° north from 15.2 to 0.6 LT, in perfect agreement with the dips indicating the presence of elliptical polarization. The methods for identifying elliptically polarized SKR in the two-antenna data do not work properly at close distances. For the goniometer inversion an SKR source approximately located 1 R_S above the pole is off by 20° from the center of Saturn when Cassini is located around 5.5 R_S (in the equatorial region). Hence ellipticity might be indicated even for circularly polarized SKR when Cassini is close to Saturn. The bottom panel of Figure 11 shows a significant drop in the fraction of circularly polarized SKR data points within ~5 R_S that can be attributed to this effect. Similarly, the polarimeter inversion (gray line) can also pretend ellipticity for a close spacecraft.

[24] We calculated the linear polarization of SKR data points for each hour from 1 September 2006 until 31 May 2007 as described above for Figure 10. The mean linear polarization of SKR and its standard deviation for observational latitudes $|\lambda_{s/c}| < 30°$ are 0.13 ± 0.09, i.e., this SKR is practically circularly polarized except some elliptical SKR polarization observed between 25° and 30° in latitude. The values for the transitional latitudes from 30° to 45° north are 0.52 ± 0.22, and the high standard deviation can be

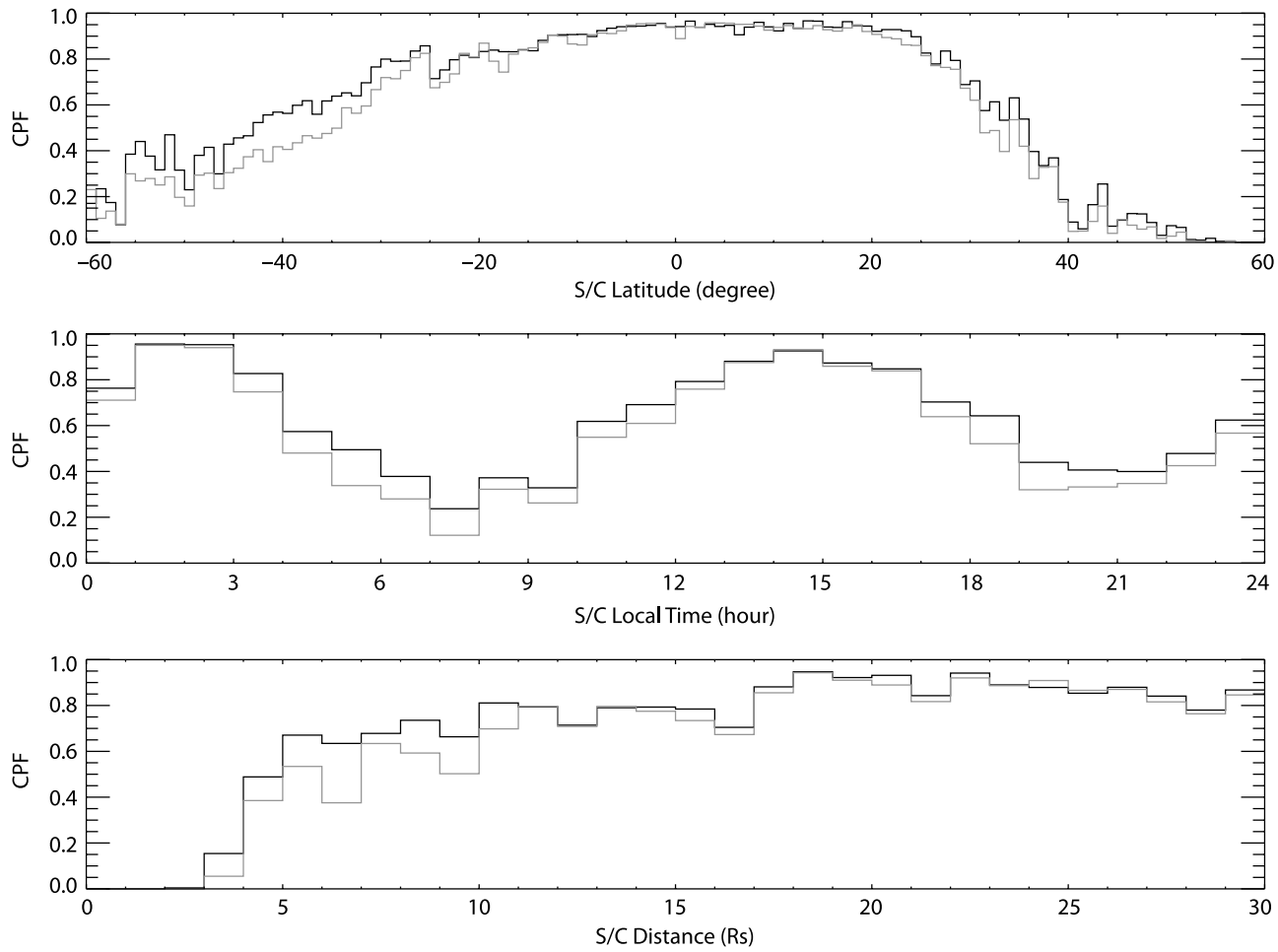

Figure 11. The circularly polarized SKR data samples fraction (CPF) as (top) a function of latitude, (middle) spacecraft local time, and (bottom) distance. The black line identifies elliptically polarized SKR as data points whose incoming directions are more than 20° off from Saturn when using the circular goniometer inversion. The gray line uses a threshold of 0.2 for the linear SKR polarization in the polarimeter inversion with the center of Saturn as preset source direction. Data selection criteria are given in the text.

attributed to the fact that circularly as well as elliptically polarized SKR can be found there. For the southern latitudes of 30° to 60° the mean linear polarization is 0.42 ± 0.18, again indicating a simultaneous presence of elliptically and circularly polarized SKR as well as a somewhat smaller degree of linear polarization. For latitudes exceeding 45° north (but below 60°) the mean linear polarization is 0.70 ± 0.12. This corresponds to a polarization ellipse with an axial ratio of about 2.4 to 1.

[25] We note that we systematically inspected all apparent polarization spectra (like in Figures 3 and 4) throughout Cassini's tour, and we could not find any significant elliptical polarization of SKR before September 2006, when the spacecraft latitude was always less than 30° in magnitude.

7. Discussion

7.1. Polarization of Nonthermal Auroral Radio Emissions

[26] The polarization aspects of planetary radio emissions were reviewed by *Lecacheux* [1988], and more recently by *Zarka* [1998]. The nonthermal auroral radio emissions of the five radio planets (Earth, Jupiter, Saturn, Uranus, Neptune) were thought to be highly circularly polarized radio waves, with the exceptions of Jupiter's decametric radiation (DAM) including S-bursts [*Queinnec and Zarka*, 2001], and the so-called bursty high latitude emission (BHL [*Reiner et al.*, 1995]). A lot of polarization measurements of planetary radio emissions have been done either with only 2 antennas on a 3-axes stabilized spacecraft (e.g., Voyagers) or with 1 or 2 antennas on a spinning spacecraft. Since the wire antennas on spacecraft have a low directivity and the direction of arrival of the radio wave is a priori unknown, only few spacecraft experiments have provided an unambiguous measurement of all four Stokes parameters so far. One of them is Cassini/RPWS and another example is the Interball-2/Polrad triaxial polarimeter, with which *Panchenko et al.* [2008] recently investigated the polarization properties of terrestrial Auroral Kilometric Radiation (AKR). They found that AKR is mostly circular, with a possible small linear component and an unpolarized component, both at a level of ~0.1. However, their measurement error is too large for a definite conclusion on the presence

or absence of a linear or unpolarized component. With respect to this study (that is limited to latitudes below 60°) it is important to note that the AKR measurements described by *Panchenko et al.* [2008] were performed at invariant northern latitudes of 62° to 82°. The Ulysses/URAP radio receiver can also measure the complete state of polarization [*Stone et al.*, 1992]. Interestingly, *Reiner et al.* [1995] have found elliptically polarized bursty radio emissions from Jupiter at frequencies of a few 100 kHz when Ulysses was at high Jovigraphic latitudes (≥30° north or south of the *magnetic* equator). This is a remarkable similarity to the occurrence of elliptically polarized SKR found in this paper. (At Saturn the magnetic latitude is practically identical to the geographic latitude.) Despite being in the same frequency range as Jovian hectometric (HOM) emission, *Reiner et al.* [1995] termed this radiation bursty high-latitude (BHL) emission, since it was observed to be more time variable than HOM and the observational Jovian longitude was generally at a range where HOM had not been observed before. The BHL emission was observed by Ulysses only at high magnetic latitudes, and it was consistently observed to be elliptically polarized, which is somewhat different to the occurrence of elliptically polarized SKR. The polarization of Jovian HOM had been found to be practically 100% circularly polarized [*Ortega-Molina and Lecacheux*, 1991]. However, this conclusion was drawn from Voyager 1 and 2 PRA observations that were performed from low magnetic latitudes barely reaching ±15°.

7.2. Possible Reasons for the Elliptical Polarization of SKR

[27] We discuss the elliptical polarization of SKR in view of Jupiter's DAM emission, which has long been known to be elliptically polarized [*Zarka*, 1998]. For example, *Lecacheux et al.* [1991] performed complete Stokes polarimetry with ground-based observations in the frequency range of 15 to 38 MHz, and a more comprehensive study with more events was later performed by *Dulk et al.* [1994]. Both found 100% elliptically polarized radiation over the entire frequency range for several hours. According to *Melrose and Dulk* [1991] the axial ratio T of the X-mode emission from the CMI process depends on the angle θ between the wave vector and the magnetic field, and it can be approximated at first order by $T \approx \cos\theta$. Since CMI theory suggests large emission angles, the wave at the source should have a large ellipticity. *Lecacheux* [1988] suggested that the elliptical polarization of Jovian DAM is directly generated by the CMI mechanism in the source and that the very low electron density close to the source leads to strong mode coupling that is retained all the way to the observer. This means that the so-called coupling parameter ψ is very large compared to $\Delta n = |n_O - n_X|$, the difference between the refractive indices of the ordinary and extraordinary mode. ψ can be seen as an expression for the rate at which the polarization of one characteristic mode changes [*Budden*, 1952]. For a very low electron density N_e it can be seen from Appleton's equation that Δn is very small. *Lecacheux* [1988] estimated that the elliptical polarization can only be retained (wave propagates as if no magnetic field is present) by a very low electron number density $N_e \leq 5$ cm^{-3} in Jupiter's magnetosphere at the source region. Later, *Melrose and Dulk* [1991] theoretically confirmed the plausibility of this estimation for the source region of Jovian DAM. However, this estimation is related to a wave frequency $f = 30$ MHz, and the required low electron density gets smaller at lower frequencies: For an emission with $f \leq 1$ MHz like SKR, *Melrose and Dulk* [1991] estimated the required density to be $N_e \leq 0.01$ cm^{-3}. RPWS measurements of auroral hiss emissions indicate that such low electron densities could exist in Saturn's magnetosphere. An electron density $N_e \leq 0.01$ cm^{-3} corresponds to an electron plasma frequency of $f_p \leq 900$ Hz, and on DOY 336, 2006, with Cassini at high latitudes, the upper frequency limit of auroral hiss was around a few hundred Hz from about 16–18 SCET. So possibly there is also strong mode coupling at the SKR source.

[28] *Lecacheux et al.* [1991] argue that there is no change in polarization in the Io torus, because the observed constant elliptical polarization of Jovian DAM is in conflict with the variability of the plasma inside the Io torus. In contrast to that, the polarization of SKR is much more variable and does depend on the latitude of the observer. Hence there might be other regions in Saturn's magnetosphere further away from the source that are so-called "limiting regions" where the "limiting polarization" is fixed, as it was previously thought to be the case for Jovian DAM by *Goertz* [1974]. The polarization that is finally observed by the antennas of the spacecraft is determined in the so-called "limiting polarization zone" (LPZ), where Δn is of the order of ψ. The difficulty in the theory of limiting polarization [*Budden*, 1952] is finding the LPZ for SKR propagating through Saturn's magnetosphere. This requires the knowledge of the electron density and the magnetic field along the raypaths, and then the coupling parameter ψ, which depends on the gradient of electron density and collision frequency, has to be determined. The limiting polarization region can then be found where the spatial change in characteristic polarization compares to the phase difference between the modes. *Sawyer et al.* [1991] estimated the limiting polarization in the LPZ for smooth Uranian radio emissions propagating from a modeled source to the Voyager 2 spacecraft. A similar investigation should be performed for SKR in Saturn's magnetosphere. This might clarify the point if the SKR polarization is fixed at the source via strong mode coupling or during propagation through a LPZ that could be a few Saturn radii away from the source.

[29] In a different theory, *Shaposhnikov et al.* [1998] suggested that moderate linear mode coupling takes place in the Jovian magnetosphere outside the source region of Jovian DAM radiation. The elliptical polarization should be formed in the so-called "transitional region," which has been applied in studies of solar radio emissions by *Zheleznyakov* [1970]. For effective coupling the ray should go through a region of quasitransverse propagation where the angle of the magnetic field $\vec{B}$ to the $\vec{k}$-vector passes 90°. There is the possibility that SKR goes through such a region if it is generated on the opposite side of the auroral region as seen from the spacecraft. Three-antenna direction-finding studies from very high latitudes in combination with ray-tracing calculations may show if this is the case or not.

[30] The visible aurora of Saturn suggests that SKR is emitted from a broad region of local times, and the observer has to be on the surface of the emission cone. *Cecconi et al.* [2009] have measured apparent SKR beaming angles (cone half angles) around 65°, but the real value could be higher when refraction is included. When SKR is observed from a spacecraft at higher observational latitude, the source region is normally not in the meridian plane, because in this case the observer looks into the hollow emission cone. The SKR source is rather on the left or right side of Saturn at local times shifted by several hours (typically 3 to 5) from the meridian plane. From there, the radio waves might travel in regions of low electron density (maybe along a potential auroral cavity) and retain their elliptical polarization due to strong mode coupling. The interpretation of FAST data (Fast Auroral SnapshoT explorer) indicates that there could be essentially zero cold electrons in the terrestrial auroral cavity [*McFadden et al.*, 1999]. This implies that the magneto-ionic theory is irrelevant in the source region. If this is the case also at Saturn, the SKR would have the CMI intrinsic elliptical polarization over a broad frequency range. However, this also poses the question why no elliptical polarization has been detected so far for Terrestrial Kilometric Radiation. On the contrary to that, SKR beamed to lower latitudes rather comes from sources close to the meridian plane. This behavior can be seen in the movie provided as supplementary material by *Cecconi et al.* [2009]. Those radio waves might then travel through a quasilongitudinal region with a higher electron density of the order of 1 planetary radius, where their polarization gets circular. It is not clear where exactly this circularization takes place and if Saturn's plasma disc also plays a role in it. Interestingly, parts of the f_p = 5 kHz boundary of the plasma disc coincide with parts of the boundary latitude of ±30° as drawn in Figure 9. Occasionally SKR goes down to such a low frequency, and thereby triggers the occurrence of periodic 5 kHz narrowband emissions [*Louarn et al.*, 2007]. The hemispherical asymmetry in the occurrence of elliptically polarized SKR shown in Figure 11 could be due to Saturn's magnetic field offset resulting also in different beaming angles for northern and southern SKR [*Cecconi et al.*, 2009]. Another reason might be a seasonally asymmetric plasma distribution.

[31] Finally, it would be good to shift away from the paradigm of circularly polarized auroral radio emissions with elliptical polarization as being exceptional. If the CMI mechanism creates elliptically polarized radio waves according to *Melrose and Dulk* [1991], we should rather ask why and where exactly they get circularized.

8. Conclusions and Outlook

[32] We have presented the first measurements of strongly elliptically polarized SKR observed from high latitudes. This discovery has already led to a change in the instrument mode of the RPWS HFR. When Cassini is at latitudes above ~30°, the three-antenna direction-finding mode is now used most of the time to determine polarization and incoming wave direction without any further assumption. Cassini has again gone to orbits with higher inclinations at the beginning of 2008. Elliptical polarization was again observed, but in this paper we restricted our analysis to the period from September 2006 to May 2007. Further experimental and theoretical investigations about this peculiar phenomenon should and will be performed. Among these could be an analysis of the tilt of the polarization ellipse as a function of frequency, a search for Faraday rotation, a tracking of the SKR source from high latitudes by three-antenna direction-finding, or identification of the limiting polarization zone or the transitional region in Saturn's magnetosphere along various raypaths of SKR.

Appendix A: Derivation of the Equations for Apparent Polarization for the RPWS Dipole-Monopole Mode

[33] An electromagnetic wave from any direction with respect to the antenna plane will generally induce the voltage $V_x = E_1\, h_x$ in the dipole antenna E_x and the voltage $V_w = E_2 h_w$ in the monopole E_w. E_1 and E_2 are simply the components of the wave electric field along these 2 quasi-perpendicular antennas, whose effective lengths are h_x and h_w, respectively. The following 4 quantities are now measured instantaneously by RPWS:

$$A_{xx} = \langle V_x V_x^* \rangle = \langle E_1 E_1^* \rangle h_x^2 \tag{A1}$$

$$A_{ww} = \langle V_w V_w^* \rangle = \langle E_2 E_2^* \rangle h_w^2 \tag{A2}$$

$$C_{xw}^r = Re\langle V_x V_w^* \rangle = Re\langle E_1 E_2^* \rangle h_x h_w = Re\langle E_2 E_1^* \rangle h_x h_w \tag{A3}$$

$$C_{xw}^i = Im\langle V_x V_w^* \rangle = Im\langle E_1 E_2^* \rangle h_x h_w = -Im\langle E_2 E_1^* \rangle h_x h_w \tag{A4}$$

A_{xx} is the autocorrelation of the dipole E_x, A_{ww} is the autocorrelation of the monopole E_w, and C_{xw}^r and C_{xw}^i are the real and imaginary parts of the cross correlation between E_x and E_w, respectively. The brackets $\langle \ldots \rangle$ represent the time averaging operation over the receiver integration time, the asterisk * denotes the complex conjugate, and the effective lengths are real quantities for the SKR frequency range (short antenna approximation). In coherency theory [*Born and Wolf*, 1999] the Stokes vector is related to the coherency vector by the following equation [*Hamaker et al.*, 1996]:

$$\begin{pmatrix} S_{app} \\ S_{app} q_{app} \\ S_{app} u_{app} \\ S_{app} v_{app} \end{pmatrix} = \begin{pmatrix} 1 & 0 & 0 & 1 \\ 1 & 0 & 0 & -1 \\ 0 & 1 & 1 & 0 \\ 0 & -i & i & 0 \end{pmatrix} \begin{pmatrix} \langle E_1 E_1^* \rangle \\ \langle E_1 E_2^* \rangle \\ \langle E_2 E_1^* \rangle \\ \langle E_2 E_2^* \rangle \end{pmatrix} \tag{A5}$$

Since E_1 and E_2 are components in the antenna plane (and not in the wave plane!), we have to set up the Stokes vector with the apparent flux and the apparent Stokes parameters

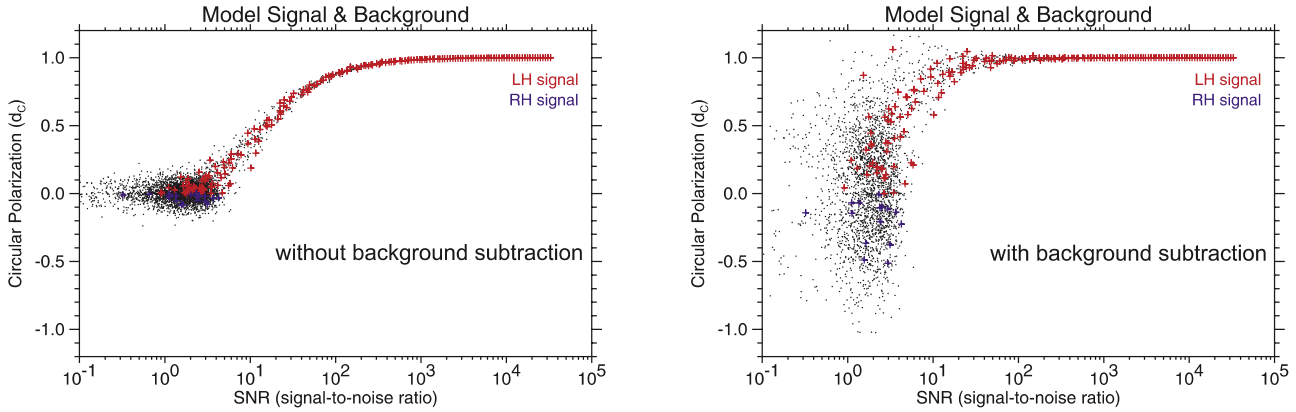

Figure B1. Model calculation of the degree of circular polarization d_c for all spectral points (black dots) and signal points (red or blue plus signs) as a function of signal-to-noise ratio (SNR). The incoming wave direction is the $-y$ direction in the Cassini s/c-frame. For the modeled autocorrelations we plot the case of (left) no background subtraction and (right) with the subtraction of the 5% occurrence level background.

(and not with the real ones!). With all the equations above it is now elementary to relate the apparent Stokes parameters to the measurement values:

$$\begin{aligned}
S_{app} &= \langle E_1 E_1^* \rangle + \langle E_2 E_2^* \rangle = \frac{\langle V_x V_x^* \rangle}{h_x^2} + \frac{\langle V_w V_w^* \rangle}{h_w^2} \\
S_{app} q_{app} &= \langle E_1 E_1^* \rangle - \langle E_2 E_2^* \rangle = \frac{\langle V_x V_x^* \rangle}{h_x^2} - \frac{\langle V_w V_w^* \rangle}{h_w^2} \\
S_{app} u_{app} &= \langle E_1 E_2^* \rangle + \langle E_2 E_1^* \rangle \\
&= Re\langle E_1 E_2^* \rangle + i\, Im\langle E_1 E_2^* \rangle + Re\langle E_2 E_1^* \rangle + i\, Im\langle E_2 E_1^* \rangle \\
&= 2Re\langle E_1 E_2^* \rangle = \frac{2Re\langle V_x V_w^* \rangle}{h_x h_w} \\
S_{app} v_{app} &= -i\langle E_1 E_2^* \rangle + i\langle E_2 E_1^* \rangle \\
&= -iRe\langle E_1 E_2^* \rangle + Im\langle E_1 E_2^* \rangle + iRe\langle E_2 E_1^* \rangle - Im\langle E_2 E_1^* \rangle \\
&= 2Im\langle E_1 E_2^* \rangle = \frac{2Im\langle V_x V_w^* \rangle}{h_x h_w}
\end{aligned} \tag{A6}$$

We only rearrange those equations to gain the following formulas:

$$\begin{aligned}
S_{app} &= \frac{A_{xx}}{h_x^2} + \frac{A_{ww}}{h_w^2} = \frac{h_w^2 A_{xx} + h_x^2 A_{ww}}{h_x^2 h_w^2} \\
q_{app} &= \left(\frac{A_{xx}}{h_x^2} - \frac{A_{ww}}{h_w^2} \right) \frac{1}{S_{app}} = \frac{h_w^2 A_{xx} - h_x^2 A_{ww}}{h_w^2 A_{xx} + h_x^2 A_{ww}} = \frac{A_{xx} - \frac{h_x^2}{h_w^2} A_{ww}}{A_{xx} + \frac{h_x^2}{h_w^2} A_{ww}} \\
u_{app} &= \frac{2C_{xw}^r}{h_x h_w} \frac{1}{S_{app}} = \frac{2C_{xw}^r h_x h_w}{h_w^2 A_{xx} + h_x^2 A_{ww}} = \frac{2C_{xw}^r \frac{h_x}{h_w}}{A_{xx} + \frac{h_x^2}{h_w^2} A_{ww}} \\
v_{app} &= \frac{2C_{xw}^i}{h_x h_w} \frac{1}{S_{app}} = \frac{2C_{xw}^i h_x h_w}{h_w^2 A_{xx} + h_x^2 A_{ww}} = \frac{2C_{xw}^i \frac{h_x}{h_w}}{A_{xx} + \frac{h_x^2}{h_w^2} A_{ww}}
\end{aligned} \tag{A7}$$

The physical units of all four RPWS measurement values A_{xx}, A_{ww}, C_{xw}^r, and C_{xw}^i are V^2/Hz. We note that for the calculation of the apparent polarization (Figures 3 and 4) no background subtraction was done for the auto and cross correlations. The apparent flux is gained by adding the fluxes from both antennas, whereas the difference of the fluxes represents the Stokes parameter q_{app}. The apparent linear polarization is also determined by the real part of the cross correlation, which is proportional to the cosine of the phase difference between the two linear components of the polarized part of the wave on both antennas. The apparent circular polarization is determined by the imaginary part of the cross correlation, which is proportional to the sine of the phase difference. It is possible to express the three apparent Stokes parameters (but not the flux) as a function of the ratio of the effective lengths of the two antennas. *Cecconi et al.* [2009] have recently made an antenna calibration improvement: they showed that the ratio $\frac{h_x}{h_w} = 2.00 \pm 0.16$ for bands ABC of the HFR, but it is $\frac{h_x}{h_w} = 2.45 \pm 0.28$ for the H1 band. We use these ratios in our calculation of the apparent polarization.

Appendix B: Simulation of the Influence of an Unpolarized Background on a Polarized Signal

[34] The influence of unpolarized background radiation on the polarization of a monochromatic signal is modeled as a function of the signal-to-noise ratio (SNR) as seen by the Cassini RPWS antenna system. This is done in order to demonstrate that elliptically polarized SKR seen in the data can also be attributed to a low SNR and that a proper background subtraction or strong signals are essential for a polarization analysis. We assume the monochromatic signal to be 100% circularly polarized in the LH sense. The unpolarized background radiation is generated under the following simplifying assumptions:

[35] 1. Only background radiation entering the antennas from outside (galactic background) is considered.

[36] 2. The intensity of the background is uniform with regard to the direction of incidence, i.e., it is assumed to be isotropic.

[37] 3. The intensity of the background is not a function of frequency. Thus the spectrum of the background consists of *white noise*.

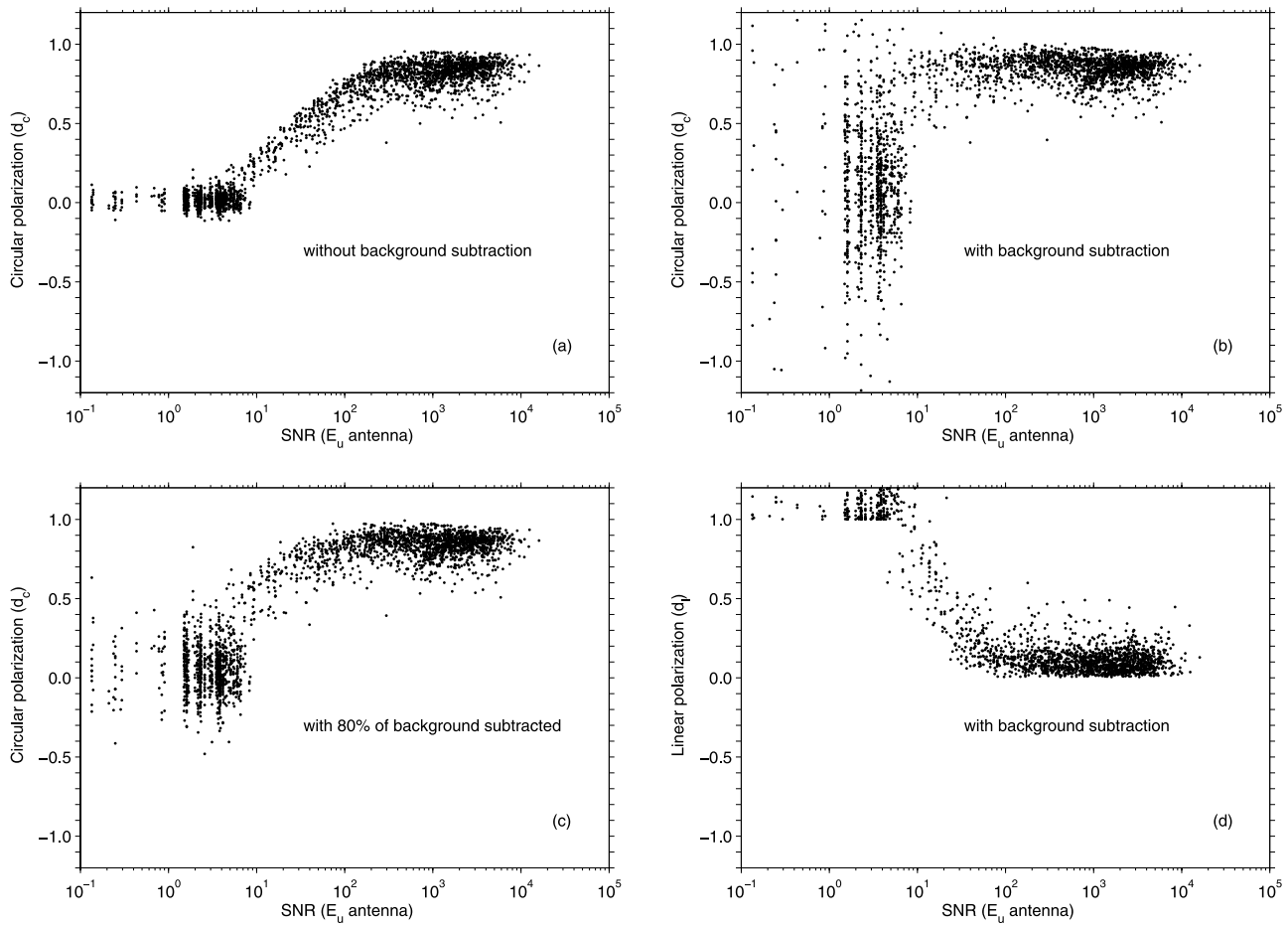

Figure B2. Circular polarization d_c and linear polarization d_l as a function of signal-to-noise ratio (SNR) of RPWS data from DOY 197, 2004, 10–11 SCET in the frequency interval from 45 to 975 kHz. The four panels show (a) d_c in case without a background subtraction, (b) d_c in case with background subtraction, (c) d_c for subtracting only 80% of the background (from the autocorrelations before the DF inversion), and (d) d_l in case with background subtraction.

[38] 4. The fluctuations of the components of the electric field vector $\vec{E}$ in the background are random according to a Gaussian distribution function. This simplifying assumption is just a first-order approximation to real conditions but serves our purpose to obtain a totally unpolarized background.

[39] 5. Generated random values for $\vec{E}$ which exceed the limit $|\vec{E}| > \mu + 3\,\sigma$ (mean plus 3 standard deviations) are set to 0 because they would produce unrealistic high background intensities. Our simulated background has a standard deviation (noise) σ of $\sim$10% of the background level. (For RPWS at a typical SKR frequency around 200 kHz the background signal intensity is $\sim 10^{-16}$ V^2/Hz with $\sigma \approx 10^{-17}$ V^2/Hz.)

[40] At the three Cassini/RPWS monopole antennas the voltages induced by the monochromatic signal and the background superpose. As a next step, these sums of voltages are taken to compute autocorrelation and cross correlation products by means of P. D. Welch's method of periodogram averaging [*Welch*, 1967]. Finally, auto and cross correlations are input to a direct inversion of the direction finding algorithm yielding the Stokes parameters *S*, *Q*, *U*, and *V*. In a first case, auto and cross correlations are left unchanged before the inversion. In a second case, the background level is subtracted from the autocorrelations (but not from the cross correlations) before the inversion. For this simulation the background was determined as the intensity at the 5% occurrence level in an intensity histogram.

[41] The degree of circular polarization d_c as a function of the signal-to-noise ratio is presented in Figure B1. The intensity of the monochromatic signal is varied over a large range of signal-to-noise ratios (SNR). Black dots comprise all spectral points. Those belonging especially to the signal are highlighted as red (or blue in case of $d_c < 0$) plus signs. As can be seen, in the first case without background subtraction the true d_c of 1 is only evident for highest signal intensities with a SNR of at least 200 (23 dB). For signal intensities close to the background level, the original state of 100% circular LH polarization is destroyed, and the signal shows a lower circular polarization. This is not the case for our second simulation performed with a background subtraction before the inversion, where the true d_c of 1 is conserved even for weak signals. We note that we assumed an incoming radio wave from the $-y$ direction of the Cassini s/c-frame, which represents a high elevation source with respect to the antenna plane.

[42] For comparison we plot real RPWS HFR data from 45 to 975 kHz of one hour from 10 to 11 SCET, DOY 197, 2004. In this time interval Cassini was located at a distance of 89 R_S and at a latitude of 17° south. Southern LH circularly polarized SKR was observed up to 600 kHz in three-antenna DF mode, and we plot the circular and linear polarization as a function of the signal-to-noise ratio in Figure B2. It can be seen that without background subtraction the real circular polarization of $d_c \sim 1$ is reached only for high values of the SNR of at least 200 or greater, similar to our model. This changes radically when a proper background subtraction is applied, and again, like in the model, a correct value for the circular polarization can be gained also for relatively weak signals. We have also drawn an intermediate case, where only 80% of the background was subtracted (corresponding to −1 dB). We note that the case of only 50% of the background subtracted (−3 dB, not drawn here) looks relatively similar to the case without any background subtraction. Since case (c) of Figure B2 still gives relatively reasonable results for weak signals, we conclude that a precise background determination with an accuracy of about 1 dB is essential for the correct determination of the circular polarization of weak signals. Figure B2d shows that the linear polarization has low values down to an SNR ≈ 20.

[43] Finally, we provide the definition of the signal-to-noise ratio (SNR) as it was used here. We also want to emphasize the difference between the SNR and the signal-to-background ratio (SBR). The SBR is simply defined as the measured signal intensity P_{sig} (in V^2/Hz) divided by the background intensity P_{bg} ($SBR = \frac{P_{sig}}{P_{bg}}$), and the signal intensity P_{sig} is the measured intensity P_{meas} minus the background intensity P_{bg}, i.e., $P_{sig} = P_{meas} - P_{bg}$. On the contrary, the signal-to-noise ratio (SNR) is calculated in the following way:

$$SNR = \frac{P_{meas} - P_{bg}}{\frac{P_{bg}}{\sqrt{\Delta f \Delta t}}} \tag{B1}$$

With Δf as the effective bandwidth and Δt as the effective integration time, the denominator of the equation above is close to the standard deviation of the background fluctuation (noise). Depending on the HFR receiver settings, typical values for $\sqrt{\Delta f \Delta t}$ lie between 10 and 20, e.g., for the DF mode in HF1 we often have $\sqrt{25\ \text{kHz}\ 16\ \text{ms}} = 20$ (the effective integration time here is ∼20% of the nominal integration time 80 ms). A simple calculation shows that $SNR = SBR\ \sqrt{\Delta f \Delta t}$, which means that the signal-to-noise ratio is typically a factor of 10–20 (10–13 dB) higher than the signal-to-background ratio. This explains why in the previous Figures 7 and B2 points of the background go up to an SNR of 10 and higher.

[44] **Acknowledgment.** The work on this paper was started when G. F. was a Postdoctoral Research Scholar at the University of Iowa, and it was finished at the Space Research Institute of the Austrian Academy of Sciences. G. F. thanks the Department of Physics and Astronomy of the University of Iowa for taking over the full publication costs. G. F. dedicates this paper to the memory of Gernot Rieger, a great artist and friend who died on 11 July, 2009.

[45] Amitava Bhattacharjee thanks Donald B. Melrose and Jan Hanasz for their assistance in evaluating this paper.

References

Boischot, A., Y. Leblanc, A. Lecacheux, B. M. Pedersen, and M. L. Kaiser (1981), Arc structure in Saturn's radio dynamic spectra, *Nature*, *292*, 727–728.

Born, M., and E. Wolf (1999), *Principles of Optics*, 7th ed., Cambridge Univ. Press, Cambridge, U. K.

Budden, K. G. (1952), The theory of limiting polarization of radio waves reflected from the ionosphere, *Proc. R. Soc.*, *215*, 1121, 215–233.

Cecconi, B., and P. Zarka (2005), Direction finding and antenna calibration through analytical inversion of radio measurements performed using a system of two or three electric dipole antennas on a three-axis stabilized spacecraft, *Radio Sci.*, *40*, RS3003, doi:10.1029/2004RS003070.

Cecconi, B., P. Zarka, and W. S. Kurth (2006), SKR polarization and source localization with the Cassini/RPWS/HFR instrument: First results, in *Planetary Radio Emissions VI*, edited by H. O. Rucker, W. S. Kurth, and G. Mann, pp. 37–49, Austrian Academy of Sciences Press, Vienna.

Cecconi, B., L. Lamy, P. Zarka, R. Prangé, W. S. Kurth, and P. Louarn (2009), Goniopolarimetric study of the revolution 29 perikrone using the Cassini Radio and Plasma Wave Science instrument high-frequency radio receiver, *J. Geophys. Res.*, *114*, A03215, doi:10.1029/2008JA013830.

Dulk, G. A., Y. Leblanc, and A. Lecacheux (1994), The complete polarization state of Io-related radio storms from Jupiter: A statistical study, *Astron. Astrophys.*, *286*, 683–700.

Fischer, G., D. A. Gurnett, A. Lecacheux, W. Macher, and W. S. Kurth (2007), Polarization measurements of Saturn Electrostatic Discharges with Cassini/RPWS below a frequency of 2 MHz, *J. Geophys. Res.*, *112*, A12308, doi:10.1029/2007JA012592.

Galopeau, P. H. M., P. Zarka, and D. Le Quéau (1995), Source location of Saturn's kilometric radiation: The Kelvin-Helmholtz instability hypothesis, *J. Geophys. Res.*, *100*(E12), 26,397–26,410.

Galopeau, P. H. M., M. Y. Boudjada, and A. Lecacheux (2007), Spectral features of SKR observed by Cassini/RPWS: Frequency bandwidth, flux density and polarization, *J. Geophys. Res.*, *112*, A11213, doi:10.1029/2007JA012573.

Goertz, C. K. (1974), Polarization of Jovian decametric radiation, *Planet. Space Sci.*, *22*, 1491–1500.

Gurnett, D. A., et al. (2004), The Cassini radio and plasma wave science investigation, *Space Sci. Rev.*, *114*, 395–463.

Hamaker, J. P., J. D. Bregman, and R. J. Sault (1996), Understanding radio polarimetry: I. Mathematical foundations, *Astron. Astrophys. Suppl.*, *117*, 137–147.

Kaiser, M. L., M. D. Desch, J. W. Warwick, and J. B. Pearce (1980), Voyager detection of nonthermal radio emission from Saturn, *Science*, *209*, 1238–1240.

Kaiser, M. L., M. D. Desch, W. S. Kurth, A. Lecacheux, F. Genova, B. M. Pedersen, and D. R. Evans (1984), Saturn as a radio source, in *Saturn*, edited by T. Gehrels and M. S. Matthews, pp. 378–415, Univ. of Ariz. Press, Tucson.

Kraus, J. D. (1986), *Radio Astronomy*, 2nd ed., Cygnus-Quasar Books, Powell, Ohio.

Lamy, L., P. Zarka, B. Cecconi, S. Hess, and R. Prangé (2008a), Modeling of Saturn Kilometric Radiation arcs and equatorial shadow zone, *J. Geophys. Res.*, *113*, A10213, doi:10.1029/2008JA013464.

Lamy, L., P. Zarka, B. Cecconi, R. Prangé, W. S. Kurth, and D. A. Gurnett (2008b), Saturn Kilometric Radiation: Average and statistical properties, *J. Geophys. Res.*, *113*, A07201, doi:10.1029/2007JA012900.

Lecacheux, A. (1988), Polarization aspects from planetary radio emissions, in *Planetary Radio Emissions II*, edited by H. O. Rucker, S. J. Bauer, and B. M. Pedersen, pp. 299–313, Austrian Acad. of Sciences Press, Vienna.

Lecacheux, A., A. Boischot, M. Y. Boudjada, and G. A. Dulk (1991), Spectra and complete polarization state of two, Io-related, radio storms from Jupiter, *Astron. Astrophys.*, *251*, 339–348.

Louarn, P., et al. (2007), Observation of similar radio signatures at Saturn and Jupiter: Implications for the magnetospheric dynamics, *Geophys. Res. Lett.*, *34*, L20113, doi:10.1029/2007GL030368.

McFadden, J. P., C. W. Carlson, R. E. Ergun, D. M. Klumpar, and E. Moebius (1999), Ion and electron characteristics in auroral density cavities associated with ion beams: No evidence for cold ionospheric plasma, *J. Geophys. Res.*, *104*(A7), 14,671–14,682.

Melrose, D. B., and G. A. Dulk (1991), On the elliptical polarization of Jupiter's decametric radio emission, *Astron. Astrophys.*, *249*, 250–257.

Ortega-Molina, A., and G. Daigne (1984), Polarization response of two crossed monopoles on a spacecraft, *Astron. Astrophys.*, *130*, 301–310.

Ortega-Molina, A., and A. Lecacheux (1990), Polarization response of the Voyager-PRA experiment at low frequencies, *Astron. Astrophys.*, *229*, 558–568.

Ortega-Molina, A., and A. Lecacheux (1991), Polarization of Jovian Hectometric Emission, *J. Geophys. Res.*, *96*(A7), 11,441–11,453.

Panchenko, M., J. Hanasz, and H. O. Rucker (2008), Estimation of linear wave polarization of the auroral kilometric radiation, *Radio Sci.*, *43*, RS1006, doi:10.1029/2006RS003606.

Queinnec, J., and P. Zarka (2001), Flux, power, energy and polarization of Jovian S-bursts, *Planet. Space Sci.*, *49*, 365–376.

Reiner, M. J., M. D. Desch, M. L. Kaiser, R. Manning, J. Fainberg, and R. G. Stone (1995), Elliptically polarized bursty radio emissions from Jupiter, *Geophys. Res. Lett.*, *22*(4), 345–348.

Sawyer, C. B., K. L. Neal, and J. W. Warwick (1991), Polarization model applied to Uranian radio emission, *J. Geophys. Res.*, *96*(A4), 5575–5590.

Shaposhnikov, V. E., Vl. V. Kocharovskii, V. V. Kocharovskii, H. P. Ladreiter, H. O. Rucker, and V. V. Zaitsev (1998), Effect of limiting polarization in the Jovian inner magnetosphere, *Radiophys. Quantum Electron.*, *41*, 115–124.

Stone, R. G., J. L. Bougeret, J. Caldwell, P. Canu, Y. de Conchy, N. Cornilleau-Wehrlin, M. D. Desch, J. Fainberg, K. Goetz, and M. L. Goldstein (1992), The Unified Radio and Plasma wave investigation, *Astron. Astrophys. Suppl. Ser.*, *92*, 291–316.

Vogl, D. F., et al. (2004), In-flight calibration of the Cassini-Radio and Plasma Wave Science (RPWS) antenna system for direction-finding and polarization measurements, *J. Geophys. Res.*, *109*, A09S17, doi:10.1029/2003JA010261.

Warwick, J. W., et al. (1981), Planetary radio astronomy observations from Voyager 1 near Saturn, *Science*, *212*, 239–243.

Warwick, J. W., D. R. Evans, J. H. Romig, J. K. Alexander, M. D. Desch, M. L. Kaiser, M. Aubier, Y. Leblanc, A. Lecacheux, and B. M. Pedersen (1982), Planetary radio astronomy observations from Voyager 2 near Saturn, *Science*, *215*, 582–587.

Welch, P. D. (1967), The use of fast Fourier transform for the estimation of power spectra: A method based on time averaging over short, modified periodograms, *IEEE Trans. Audio Electroacoust.*, *AU-15*, 70–73.

Wu, C. S., and L. C. Lee (1979), A theory of the terrestrial kilometric radiation, *Astrophys. J.*, *230*, 621–626.

Zarka, P. (1998), Auroral radio emissions at the outer planets: Observations and theories, *J. Geophys. Res.*, *103*(E9), 20,159–20,194.

Zheleznyakov, V. V. (1970), *Radio Emission of the Sun and Planets*, Pergamon, New York.

B. Cecconi, L. Lamy, and P. Zarka, LESIA, Observatoire de Paris, 5 Place Jules Janssen, F-92190 Meudon, France.

G. Fischer, W. Macher, and U. Taubenschuss, Space Research Institute, Austrian Academy of Sciences, Schmiedlstr. 6, A-8042 Graz, Austria. (georg.fischer@oeaw.ac.at)

D. A. Gurnett, W. S. Kurth, and S.-Y. Ye, Department of Physics and Astronomy, University of Iowa, 203 Van Allen Hall, Iowa City, IA 52242, USA.